Neurocomputing 463 (2021) 483–494

Contents lists available at ScienceDirect

Neurocomputing

journal homepage: www.elsevier.com/locate/neucom

# Fixed-time adaptive observer-based time-varying formation control for multi-agent systems with directed topologies

Tianyi Xiong [a], Zhou Gu [a,*], Jianqiang Yi [b,c], Zhiqiang Pu [b,c]

[a] College of Mechanical and Electronic Engineering, Nanjing Forestry University, Nanjing 210037, China
[b] Institute of Automation, Chinese Academy of Sciences, Beijing 100190, China
[c] School of Artificial Intelligence, University of Chinese Academy of Sciences, Beijing 100049, China

ARTICLE INFO

*Article history:*
Received 1 April 2021
Revised 12 August 2021
Accepted 16 August 2021
Available online 20 August 2021
Communicated by Zidong Wang

*Keywords:*
Directed topologies
Formation control
Fixed-time observer
Multi-agent systems

ABSTRACT

In this paper, a novel time-varying formation tracking control scheme in fixed-time framework under directed topologies is proposed for multi-agent systems (MASs), with consideration of uncertainties and the absence of the leader's velocity measurements (LVMs). First, a novel cascaded fixed-time state observer (CFTSO) under directed topologies without LVMs is developed for each follower to acquire the estimates of the leader's states (LSs) in a fixed time. Then, minimal learning parameter (MLP) methods combining with radial basis function neural networks (RBFNNs) are utilized to cope with the uncertainties. Finally, on the basis of the designed CFTSO and MLP, a new formation control scheme in fixed-time framework under directed topologies is established to solve the time-varying formation tracking control problem.



## 1. Introduction

Recently, formation control problem for multi-agent systems (MASs) has been gaining popularity and obtained a wealth of achievements [1–3]. Note that the majority goals of the available formation control strategies are realizing time-invariant formation shapes. Nevertheless, such formations cannot satisfy practical application requirements when multiple obstacles need to be avoided and there exist rapid changes in external environment. Thus, increasing achievements on time-varying formation control have been made in recent decades [4–6].

Convergence rate is usually treated as a vital criterion to evaluate the formation control performance for MASs. As we all know, one of the efficient methods of improving convergence rate is to realize finite time convergence compared to asymptotic convergence. However, the settling time function derived from finite-time stability analysis grows unbounded along with the values of the initial states. For the sake of overcoming the above shortcomings, fixed-time stability emerges in [7]. Such stability property guarantees that the settling time is irrelative to the initial state values and uniformly bounded [8]. As a result of the superiority of fixed-time stability, some studies of fixed-time consensus and formation control for MASs are conducted in [9,10].

Inaccurate leader's velocity measurements (LVMs) in formation control may result in deterioration of the control performance. In practice, LVMs may be contaminated by noises [11–13]. To solve the problem, some control schemes based on velocity observers are investigated to estimate the LVMs in [13,14]. However, because of the distributed manner of MASs, only a portion of the followers can access to the state information of the leader, so that the output of the velocity observer of the leader cannot be acquired by each follower, which will bring the challenge to robust nonlinear control design and analysis. To overcome this difficulty, some researchers try to design distributed observers to provide the estimates of the LVMs for each follower in [10,15,16]. Furthermore, to improve the convergence rate of the observers and avoid the shortcoming of the finite-time control, fixed-time distributed observers for the leader's states (LSs) are established in [9,10,17]. However, most distributed leader states observers are designed under connected topologies, which means that the information sharing among the followers is bidirectional and sets high demand on the communication channel. In fact, digraph communication topology costs less resources and has a less requirement on the communication equipment [9]. Great efforts have been made in [9,17] to extend the existing results to the digraph cases, which are very meaningful. However, both the leader's position measurements (LPMs) and LVMs are indispensable [9,17]. In [11,12], cascaded fixed-time leader state observers are conducted for each follower to acquire the estimates of the LPMs and LVMs in a fixed time without LVMs.

* Corresponding author.
*E-mail address:* gzh1808@163.com (Z. Gu).

https://doi.org/10.1016/j.neucom.2021.08.081
0925-2312/

However, the communication topologies are assumed to be connected in [11,12]. Therefore, the leader state fixed-time observer design problem without the LVMs under directed topologies still remains open. It is really challenging to extend the existing results to design such an observer since the analysis of the fixed-time stability is very complex. Besides, asymmetric topology property also brings great difficulties to the observer design and stability analysis.

The existences of uncertainties [18,19], disturbance [20] and so on, may deteriorate the formation control performance, and even result in instabilities of the closed-loop formation control systems. To deal with uncertainties, radial basis function neural networks (RBFNNs) are widely utilized in the cooperative control of MASs [21–24]. Nevertheless, it should be pointed out that a huge number of adaptive parameters need to be updated online in the majority of the existing conditional RBFNN based adaptive control, which may be time-consuming and burdensome in reality. Aimed at solving this problem, minimal learning parameter (MLP) technique is adopted in [25,26] for the hypersonic vehicle control. Then, some researchers use MLP technique to deal with the uncertainty problem in the cooperative control for MASs, and to decrease the number of the adaptive parameters simultaneously [27]. However, the assumption of the boundedness of the weight error matrix's norm needs to be satisfied in [27], which may be unreasonable in theory. MLP technique is also used to deal with the uncertainty problem in [23]. However, this result only achieves the boundedness of the tracking error and severely depends on the accurate LVMs. Such situation can result in the instability of formation control system and even the failure of the formation task when the precise LVMs are difficult to obtain.

As far as we know, the problem of adaptive time-varying formation tracking control for MASs with uncertainties in fixed-time framework under directed topologies and without the LVMs still needs to be investigated. Inspired by the aforementioned facts, we propose a novel adaptive formation tracking control scheme in fixed-time framework for MASs on the basis of MLP techniques and cascaded fixed-time state observer (CFTSO) without LVMs. First, a novel CFTSO under directed topologies is designed for each follower so that each follower can acquire the estimates of the LSs without LVMs in a fixed time. Second, MLP techniques based on RBFNNs are adopted to deal with the unknown uncertainties and lessen the calculative burden simultaneously. Finally, a fixed-time adaptive control scheme with the proposed CFTSO and MLP is constructed to deal with the time-varying formation tracking control problem in presence of uncertainties and in absence of LVMs under directed topologies. The highlights of this paper can be summarized as follows:

1) The proposed formation control scheme and CFTSO are constructed under directed topologies. In fact, the majority of the existing distributed observers are established under connected topologies [10–12], where the stability analysis is much easier due to the symmetric and positive definite property of the Laplacian matrix of the connected graphs. Hence, it is really nontrivial to construct the CFTSO under directed topologies. In addition, different from the distributed fixed-time observer [9,17,28], there is no discontinuous term in the proposed CFTSO, which will not cause the chattering problem. Furthermore, since the CFTSO is constructed such that each follower can get the estimates under directed topologies within a fixed time, the whole formation control scheme can work under directed topologies. The results in [29–31] propose consensus control protocols under directed topologies. However, the control inputs of the neighbor agents are necessary, which may be hard to be implemented in practice.
2) This paper addresses the time-varying formation control problem in fixed-time framework for MASs without the LVMs. In comparison with the available fixed-time consensus and formation control scheme in [9,10,17,28,32,33], the presented fixed-time formation control scheme can also operate well without the LVMs since the novel CFTSO proposed in this paper can get the estimates of the LSs within a fixed time.
3) The proposed time-varying formation control scheme for MASs on the basis of MLP and CFTSO can realize the expected time-varying formation in a fixed time in presence of unknown uncertainties. Different from the results in [11,21,23,24], the proposed control scheme in this paper can drive the formation tracking errors to a small region around the origin within a fixed time instead of being ultimately uniformly bounded (UUB). Compared to the result in [27], the proposed formation control scheme is able to realize the fixed-time convergence for MASs with uncertainties in absence of the LVMs under directed topologies. Furthermore, the number of the adaptive parameters can be reduced to a great extent due to the application of MLP techniques. As a result, the proposed control scheme overcomes the drawbacks of the existing results and is really practical and novel.

The remainder of this paper is organized as follows. Problem description and preliminaries are introduced in Sections 2 and 3, respectively. Formation tracking control scheme design is presented in Section 4. Numerical simulation results are given in Section 5. Conclusions are drawn in Section 6.

## 2. Preliminaries

In this paper, the MASs with one leader and $N$ followers are considered. The dynamics of the $i$th follower are described as

$$\begin{cases} \dot{x}_i(t) = v_i(t), \\ \dot{v}_i(t) = f_i(x_i(t), v_i(t)) + u_i(t), \ i = 1, 2, \cdots N, \end{cases} \tag{1}$$

where $x_i(t) \in R^m$ and $v_i(t) \in R^m$ stand for the position and velocity state vectors of the $i$th follower, respectively; $m$ is the dimension of the state vectors $x_i(t) \in R^m$ and $v_i(t); u_i(t) \in R^m$ represents the control input vector; $f_i(x_i(t), v_i(t)) : R^{2m} \to R^m$ denotes an unknown and continuous function vector.

The leader is modeled as

$$\begin{cases} \dot{x}_0(t) = v_0(t), \\ \dot{v}_0(t) = u_0(t), \end{cases} \tag{2}$$

where $x_0(t) \in R^m$ and $v_0(t) \in R^m$ are position and velocity state vectors of the leader, respectively; $u_0(t) \in R^m$ represents the control input vector.

For the $i$th follower, we denote piecewise continuously differentiable function vector $h_i(t) = [h_{xi}^T(t), h_{vi}^T(t)]^T \in R^{2m}$ with $\dot{h}_{xi}(t) = h_{vi}(t)$ as the command vector, which is used to describe the expected time-varying formation shape.

Let vector $\delta_i(t) = [\delta_{xi}^T(t), \delta_{vi}^T(t)]^T \in R^{2m}$ be the formation tracking error vector, where $\delta_{xi}(t) = x_i(t) - x_0(t) - h_{xi}(t)$ and $\delta_{vi}(t) = v_i(t) - v_0(t) - h_{vi}(t)$ are formation tracking position error vector and velocity error vector, respectively. In addition, define $\delta_x(t) = [\delta_{x1}^T(t), \delta_{x2}^T(t), \ldots, \delta_{xN}^T(t)]^T$ and $\delta_v(t) = [\delta_{v1}^T(t), \delta_{v2}^T(t), \ldots, \delta_{vN}^T(t)]^T$.

The control objective of the current paper is to propose an adaptive formation tracking control scheme in fixed-time framework based on a fixed-time observer so that the formation tracking error $\delta_i(t)$ is able to converge to a small region around the origin in a fixed time under directed topologies without the LVMs, which means the expected time-varying formation of MASs (1) and (2) with uncertainties is realized in a fixed time.

Moreover, we made the following reasonable assumptions:

**Assumption 1.** $u_0(t)$ is assumed to be acquired by the followers.

**Assumption 2.** The graph $G$among the followers and the leader contains a spanning tree with the leader being the root node.

## 3. Fixed-time formation tracking control scheme design

In this section, firstly, a novel CFTSO is put forward to reconstruct the states of the leader in a fixed time. The, MLP method based on RBFNNs is utilized to cope with the uncertainties. Finally, a new formation tracking scheme based on CFTSO and MLP in fixed-time framework is established for the MASs. The block diagram of the overall formation control scheme is displayed in Fig. 1. Firstly, the CFTSO is designed for each follower to provide the estimates of the LSs in a fixed time. Then, combining the CFTSO and MLP techniques which is utilized to deal with the uncertainties, a fixed-time adaptive control law deduced by backstepping method is proposed to achieve the time-varying formation tracking in a fixed-time. In addition, for simplicity, we omit $(t)$ for all the variables in the rest of this paper.

### *3.1. Cascaded fixed-time state observer for the leader under directed topologies*

In this subsection, a new CFTSO is constructed for each follower to estimate the LSs $x_0$ and $v_0$ in a fixed time under directed topologies without the LVMs.

Let $\hat{x}_{0i}$ and $\hat{v}_{0i}$ represent the estimates of $x_0$ and $v_0$ for the $i$th follower, respectively. The CFTSO is designed as:

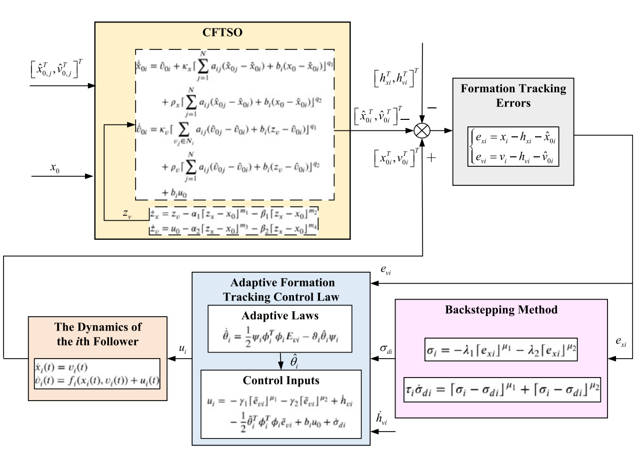


**Fig. 1.** The block diagram of the overall formation control scheme.

$$\begin{cases} \dot{\hat{x}}_{0i} = & \hat{v}_{0i} + \kappa_x \lceil \sum_{j=1}^{N} a_{ij}(\hat{x}_{0j} - \hat{x}_{0i}) + b_i(x_0 - \hat{x}_{0i}) \rfloor^{q_1} \\ & + \rho_x \lceil \sum_{j=1}^{N} a_{ij}(\hat{x}_{0j} - \hat{x}_{0i}) + b_i(x_0 - \hat{x}_{0i}) \rfloor^{q_2}, \\ \dot{\hat{v}}_{0i} = & \kappa_v \lceil \sum_{v_j \in N_i} a_{ij}(\hat{v}_{0j} - \hat{v}_{0i}) + b_i(z_v - \hat{v}_{0i}) \rfloor^{q_1} \\ & + \rho_v \lceil \sum_{j=1}^{N} a_{ij}(\hat{v}_{0j} - \hat{v}_{0i}) + b_i(z_v - \hat{v}_{0i}) \rfloor^{q_2} + u_0, \end{cases} \tag{3}$$

where the observer gains $\kappa_x, \kappa_v, \rho_x, \rho_v > 0$, the constant $q_1 > 1, q_2 < 1$. Function $\lceil x \rfloor^\alpha = |x|^\alpha \mathrm{sign}(x)$, where $\mathrm{sign}(x)$ is signum function with respect of $x$ with $x \in R$. $b_i$ denotes the information sharing between the $i$th follower and the leader. $b_i = 1$ if and only if the $i$th follower can receive the state information from the leader; otherwise $b_i = 0$. Moreover, we set $a_{ij} = 1, j \neq i$ if and only if the $j$th follower can deliver the state information to the $i$th follower; otherwise $a_{ij} = 0$. $z_v$ is the estimate of $v_0$ for the $i$th follower with $b_i = 1$, which is acquired by the following fixed-time observer:

$$\begin{cases} \dot{z}_x = z_v - \alpha_1 \lceil z_x - x_0 \rfloor^{m_1} - \beta_1 \lceil z_x - x_0 \rfloor^{m_2}, \\ \dot{z}_v = u_0 - \alpha_2 \lceil z_x - x_0 \rfloor^{m_3} - \beta_2 \lceil z_x - x_0 \rfloor^{m_4}, \end{cases} \tag{4}$$

where $z_x$ is the estimate of $x_0$ for the $i$th followers with $b_i = 1$. The observer parameters $m_1, m_2, m_3, m_4 > 0$ satisfy $m_1, m_3 \in (0,1)$, $m_2, m_4 > 1$ and $m_3 = 2m_1 - 1, m_4 = 2m_2 - 1$ with $m_1 \in (1 - \epsilon_1, 1)$ and $m_2 \in (1, 1 + \epsilon_2)$ for sufficiently small constants $\epsilon_1$ and $\epsilon_2$. Other observer gains $\alpha_1, \alpha_2, \beta_1, \beta_2 > 0$ are selected to make the matrices $A_1$ and $A_2$ meet the Hurwitz condition, where $A_1$ and $A_2$ are

$$A_1 = \begin{bmatrix} -\alpha_1 & 1 \\ -\alpha_2 & 0 \end{bmatrix}, A_2 = \begin{bmatrix} -\beta_1 & 1 \\ -\beta_2 & 0 \end{bmatrix}.$$

**Remark 1.** For the $i$th follower satisfying $b_i = 1$, only fixed-time observer (4) is needed to obtain the estimates of $x_0$ and $v_0$ within a fixed time. For the $i$th follower satisfying $b_i = 0$, the fixed-time observer (3) and (4) are necessary. Besides, the input of observer (3) $z_v$ is acquired by (4). Therefore, fixed-time observers (3) and (4) constitute the CFTSO to provide the estimates of $x_0$ and $v_0$ for each follower within a fixed time with no need for the LVMs.

**Remark 2.** Due to the cascaded structure of the proposed observer, the CFTSO consisting of (3) and (4) is able to obtain the estimates of $x_0$ and $v_0$ within a fixed time only dependent on LPMs, while both position and velocity measurements are indispensable in the fixed-time distributed observers in [9,10,17,28,32]. Note that the outputs of the observer (4) $z_x$ and $z_v$ can only be obtained by the followers which are directly accessible to the leader information, while the other followers cannot due to the distributed manner. Thus, distributed observer (3) is necessary for the $i$th follower with $b_i = 0$ since it is unreasonable to share $z_x$ and $z_v$ among the followers.

**Remark 3.** The proposed CFTSO is established under directed topologies, which is a really sounding innovation compared to the cascaded fixed-time observers in [11,12]. Furthermore, any discontinuous item does not exist in the proposed CFTSO in this paper, while discontinuous items $\mathrm{sign}(\cdot)$ exist in the fixed-time distributed observers in [9,17,28]. Therefore, the proposed CFTSO is really practical and robust in practice.

**Theorem 1.** *Suppose Assumptions 1 and 2 hold. Then, each follower can acquire the estimates of the LSs by the proposed CFTSO consisting of (3) and (4) within a fixed time.*

**Proof 1.** The proof proceeds in three steps.

**Step 1**. In this step, it will be proved that the $i$th follower with $b_i = 1$ can acquire the estimates of the LSs in a fixed time by means of observer (4). Define $\tilde{z}_x = z_x - x_0$ and $\tilde{z}_v = z_v - v_0$. Invoking (2) and (4), we can get

$$\begin{cases} \dot{\tilde{z}}_x = \tilde{z}_v - \alpha_1 \lceil \tilde{z}_x \rfloor^{m_1} - \beta_1 \lceil \tilde{z}_x \rfloor^{m_2}, \\ \dot{\tilde{z}}_v = -\alpha_2 \lceil \tilde{z}_x \rfloor^{m_3} - \beta_2 \lceil \tilde{z}_x \rfloor^{m_4}. \end{cases} \tag{5}$$

Then, on the basis of the result in [34], we can conclude that $\tilde{z}_x$ and $\tilde{z}_v$ will converge to the origin within fixed time $T_1$, which is bounded by

$$T_1 \leqslant \frac{\lambda_{\max}^{2-m_1}(P_1)}{(1-m_1)\lambda_{\min}(Q_1)} + \frac{\lambda_{\max}(P_2)}{(m_2-1)\lambda_{\min}(Q_2)\iota^{q_0-1}}, \tag{6}$$

where matrices $P_1, P_2, Q_1, Q_2$ are positive definite and satisfy $P_1 A_1 + A_1^T P_1 = -Q_1, P_2 A_2 + A_2^T P_2 = -Q_2$. Positive constant $\iota$ satisfies $\iota \leqslant \lambda_{\min}(P_2)$.

**Step 2**. Define observation errors as $\tilde{x}_{0i} = \hat{x}_{0i} - x_0$ and $\overline{v}_{0i} = \hat{v}_{0i} - v_0$. Since $z_v = v_0$ when $t \geqslant T_1$, we define auxiliary observation errors as $\tilde{x}_{0i} = \hat{x}_{0i} - x_0$ and $\tilde{v}_{0i} = \hat{v}_{0i} - z_v$. In this step, we prove that $\tilde{x}_{0i}$ and $\tilde{v}_{0i}$ are bounded at any finite time interval $[t_0, t]$. Then, the dynamics of $\tilde{x}_{0i}$ and $\tilde{v}_{0i}$ can be written as

$$\begin{cases} \dot{\tilde{x}}_{0i} = & \tilde{v}_{0i} + \kappa_x \lceil \sum_{j=1}^{N} a_{ij}(\tilde{x}_{0j} - \tilde{x}_{0i}) - b_i \tilde{x}_{0i} \rfloor^{q_1} \\ & + \rho_x \lceil \sum_{j=1}^{N} a_{ij}(\tilde{x}_{0j} - \tilde{x}_{0i}) - b_i \tilde{x}_{0i} \rfloor^{q_2}, \\ \dot{\tilde{v}}_{0i} = & \kappa_v \lceil \sum_{j=1}^{N} a_{ij}(\hat{v}_{0j} - \hat{v}_{0i}) + b_i(z_v - \hat{v}_{0i}) \rfloor^{q_1} + u_0 \\ & + \rho_v \lceil \sum_{j=1}^{N} a_{ij}(\hat{v}_{0j} - \hat{v}_{0i}) + b_i(z_v - \hat{v}_{0i}) \rfloor^{q_2} - \dot{z}_v. \end{cases} \tag{7}$$

Let vectors $\eta_x = [\tilde{x}_{01}^T, \tilde{x}_{02}^T, \ldots, \tilde{x}_{0N}^T]^T$ and $\eta_v = [\tilde{v}_{01}^T, \tilde{v}_{02}^T, \ldots, \tilde{v}_{0N}^T]^T$. Then, (7) can be written in a compact form as follows:

$$\begin{cases} \dot{\eta}_x = \eta_v - \kappa_x \lceil H\eta_x \rfloor^{q_1} - \rho_x \lceil H\eta_x \rfloor^{q_2}, \\ \dot{\eta}_v = -\kappa_v \lceil H\eta_v \rfloor^{q_1} - \rho_v \lceil H\eta_v \rfloor^{q_2} + \bar{u}_0 - \bar{z}_v, \end{cases} \tag{8}$$

where matrices $B = \mathrm{diag}\{b_i\}$ and $\bar{B} = B \otimes I_m; H = (L+B) \otimes I_m$ where $L = \mathrm{diag}\{\sum_{j=1}^{N} a_{ij}\} - A$ with $A = [a_{ij}] \in R^{N \times N}$; vectors $\bar{u}_0 = 1_N \otimes u_0$ and $\bar{z}_v = 1_N \otimes \dot{z}_v$.

In addition, we define the following local neighborhood observation errors:

$$\begin{cases} \varepsilon_{xi} = \sum_{j=1}^{N} a_{ij}(\tilde{x}_{0i} - \tilde{x}_{0j}) + b_i \tilde{x}_{0i}, \\ \varepsilon_{vi} = \sum_{j=1}^{N} a_{ij}(\tilde{v}_{0i} - \tilde{v}_{0j}) + b_i \tilde{v}_{0i}. \end{cases} \tag{9}$$

Taking the derivative of $\varepsilon_{xi}$ and $\varepsilon_{vi}$ with respect to time $t$ yields

$$\begin{cases} \dot{\varepsilon}_{xi} = & \varepsilon_{vi} - \kappa_x (\sum_{j=1}^{N} a_{ij}(\lceil \varepsilon_{xi} \rfloor^{q_1} - \lceil \varepsilon_{xj} \rfloor^{q_1}) + b_i \lceil \varepsilon_{xi} \rfloor^{q_1}) \\ & -\rho_x (\sum_{j=1}^{N} a_{ij}(\lceil \varepsilon_{xi} \rfloor^{q_2} - \lceil \varepsilon_{xj} \rfloor^{q_2}) + b_i \lceil \varepsilon_{xi} \rfloor^{q_2}), \\ \dot{\varepsilon}_{vi} = & -\kappa_v (\sum_{j=1}^{N} a_{ij}(\lceil \varepsilon_{vi} \rfloor^{q_1} - \lceil \varepsilon_{vj} \rfloor^{q_1}) + b_i \lceil \varepsilon_{vi} \rfloor^{q_1}) \\ & -\rho_v (\sum_{j=1}^{N} a_{ij}(\lceil \varepsilon_{vi} \rfloor^{q_2} - \lceil \varepsilon_{vj} \rfloor^{q_2}) + b_i \lceil \varepsilon_{vi} \rfloor^{q_2}) \\ & -b_i \dot{\tilde{z}}_v. \end{cases} \tag{10}$$

Construct the following Lyapunov function:

$$\begin{aligned} V = & \sum_{i=1}^{N} p_i (\tfrac{\kappa_x}{q_1+1} |\varepsilon_{xi}|^{q_1 T} |\varepsilon_{xi}| + \tfrac{\rho_x}{q_2+1} |\varepsilon_{xi}|^{q_2 T} |\varepsilon_{xi}|) \\ & + \sum_{i=1}^{N} p_i (\tfrac{\kappa_v}{q_1+1} |\varepsilon_{vi}|^{q_1 T} |\varepsilon_{vi}| + \tfrac{\rho_v}{q_2+1} |\varepsilon_{vi}|^{q_2 T} |\varepsilon_{vi}|) \\ = & V_1 + V_2, \end{aligned} \tag{11}$$

where $V_1 = \sum_{i=1}^{N} p_i (\frac{\kappa_x}{q_1+1} |\varepsilon_{xi}|^{q_1 T} |\varepsilon_{xi}| + \frac{\rho_x}{q_2+1} |\varepsilon_{xi}|^{q_2 T} |\varepsilon_{xi}|)$, and $V_2 = \sum_{i=1}^{N} (p_i \frac{\kappa_v}{q_1+1} |\varepsilon_{vi}|^{q_1 T} |\varepsilon_{vi}| + \frac{\rho_v}{q_2+1} |\varepsilon_{vi}|^{q_2 T} |\varepsilon_{vi}|)$. $p_i$ is defined as the $i$th element of vector $[p_1, p_2, \ldots, p_N]^T = (L+B)^{-T} 1_N$. In addition, let $P = \mathrm{diag}\{p_1, p_2, \ldots, p_N\} \otimes I_m$ and $Q = \frac{1}{2}(PH + H^T P)$. Then, according to Lemma 1 in [9], the matrices $P$ and $Q$ are both positive definite. Thus, we have

$$\begin{aligned} \dot{V} = & \sum_{i=1}^{N} p_i (\kappa_x \lceil \varepsilon_{xi} \rfloor^{q_1} + \rho_x \lceil \varepsilon_{xi} \rfloor^{q_2})^T [\varepsilon_{vi} - \kappa_x (\sum_{j=1}^{N} a_{ij} \times \\ & (\lceil \varepsilon_{xi} \rfloor^{q_1} - \lceil \varepsilon_{xj} \rfloor^{q_1}) + b_i \lceil \varepsilon_{xi} \rfloor^{q_1})] \\ & - \sum_{i=1}^{N} p_i (\kappa_x \lceil \varepsilon_{xi} \rfloor^{q_1} + \rho_x \lceil \varepsilon_{xi} \rfloor^{q_2})^T [\rho_x (\sum_{j=1}^{N} a_{ij} \times \\ & (\lceil \varepsilon_{xi} \rfloor^{q_2} - \lceil \varepsilon_{xj} \rfloor^{q_2}) + b_i \lceil \varepsilon_{xi} \rfloor^{q_2})] \\ & - \sum_{i=1}^{N} p_i (\kappa_v \lceil \varepsilon_{vi} \rfloor^{q_1} + \rho_v \lceil \varepsilon_{vi} \rfloor^{q_2})^T \times \\ & [\kappa_v (\sum_{j=1}^{N} a_{ij} (\lceil \varepsilon_{vi} \rfloor^{q_1} - \lceil \varepsilon_{vj} \rfloor^{q_1}) + b_i \lceil \varepsilon_{vi} \rfloor^{q_1})] \\ & - \sum_{i=1}^{N} p_i (\kappa_v \lceil \varepsilon_{vi} \rfloor^{q_1} + \rho_v \lceil \varepsilon_{vi} \rfloor^{q_2})^T [\rho_v (\sum_{j=1}^{N} a_{ij} \times \\ & (\lceil \varepsilon_{vi} \rfloor^{q_2} - \lceil \varepsilon_{vj} \rfloor^{q_2}) + b_i \lceil \varepsilon_{vi} \rfloor^{q_2})] \\ & - \sum_{i=1}^{N} p_i (\kappa_v \lceil \varepsilon_{vi} \rfloor^{q_1} + \rho_v \lceil \varepsilon_{vi} \rfloor^{q_2})^T b_i \dot{\tilde{z}}_v. \end{aligned}$$

By further computing, we can get

$$\begin{aligned} \dot{V} = & \sum_{i=1}^{N} p_i (\kappa_x \lceil \varepsilon_{xi} \rfloor^{q_1} + \rho_x \lceil \varepsilon_{xi} \rfloor^{q_2})^T \varepsilon_{vi} - (\kappa_x \lceil \varepsilon_x \rfloor^{q_1} \\ & + \rho_x \lceil \varepsilon_x \rfloor^{q_2})^T PH (\kappa_x \lceil \varepsilon_x \rfloor^{q_1} + \rho_x \lceil \varepsilon_x \rfloor^{q_2}) \\ & - (\kappa_v \lceil \varepsilon_v \rfloor^{q_1} + \rho_v \lceil \varepsilon_v \rfloor^{q_2})^T PH (\kappa_v \lceil \varepsilon_v \rfloor^{q_1} \\ & + \rho_v \lceil \varepsilon_v \rfloor^{q_2}) - \sum_{i=1}^{N} p_i (\kappa_v \lceil \varepsilon_{vi} \rfloor^{q_1} + \rho_v \lceil \varepsilon_{vi} \rfloor^{q_2})^T b_i \dot{\tilde{z}}_v. \end{aligned}$$

From Lemma 1 in [9], we can get that $-(\kappa_x \lceil \varepsilon_x \rfloor^{q_1} + \rho_x \lceil \varepsilon_x \rfloor^{q_2})^T PH(\kappa_x \lceil \varepsilon_x \rfloor^{q_1} + \rho_x \lceil \varepsilon_x \rfloor^{q_2}) - (\kappa_v \lceil \varepsilon_v \rfloor^{q_1} + \rho_v \lceil \varepsilon_v \rfloor^{q_2})^T \times PH(\kappa_v \lceil \varepsilon_v \rfloor^{q_1} + \rho_v \lceil \varepsilon_v \rfloor^{q_2}) \leqslant 0$. Then, the derivative of $V$ turns into

$$\begin{aligned} \dot{V} \leqslant & \sum_{i=1}^{N} p_i (\kappa_x \lceil \varepsilon_{xi} \rfloor^{q_1} + \rho_x \lceil \varepsilon_{xi} \rfloor^{q_2})^T \varepsilon_{vi} \\ & - \sum_{i=1}^{N} p_i (\kappa_v \lceil \varepsilon_{vi} \rfloor^{q_1} + \rho_v \lceil \varepsilon_{vi} \rfloor^{q_2})^T b_i \dot{\tilde{z}}_v \\ \leqslant & \gamma_1 V - \sum_{i=1}^{N} p_i (\kappa_v \lceil \varepsilon_{vi} \rfloor^{q_1} + \rho_v \lceil \varepsilon_{vi} \rfloor^{q_2})^T b_i \dot{\tilde{z}}_v. \end{aligned} \tag{12}$$

where $\gamma_1 = \beta(q_1 + 1)$ with $\beta = \frac{\max\{\kappa_x, \rho_x\}}{\min\{\kappa_x, \kappa_v, \rho_x, \rho_v\}}$. The last inequality is derived from the fact $|\varepsilon_{xi}|^{q_1 T} \varepsilon_{vi} \leqslant |\varepsilon_{xi}|^{q_1 T} |\varepsilon_{xi}| + |\varepsilon_{vi}|^{q_1 T} |\varepsilon_{vi}|$ and $|\varepsilon_{xi}|^{q_2 T} \varepsilon_{vi} \leqslant |\varepsilon_{xi}|^{q_2 T} |\varepsilon_{xi}| + |\varepsilon_{vi}|^{q_2 T} |\varepsilon_{vi}|$.

According to Step 1, $\tilde{z}_v$ is able to converge to the origin in a fixed time. Thus, $\tilde{z}_v$ is bounded all the time. Then, $b_i\|\dot{\tilde{z}}_v\|_\infty \leqslant \gamma_2$ holds for a constant $\gamma_2 > 0$. Hence, we have

$$\dot{V} \leqslant \gamma_1 V + \gamma_2 \sum_{i=1}^{N} p_i(\kappa_v\|\varepsilon_{vi}^{q_1}\|_1 + \rho_v\|\varepsilon_{vi}^{q_2}\|_1). \tag{13}$$

Let $\varepsilon_{vil}$ be the $l$th element of the vector $\varepsilon_{vi}, l = 1, 2, \ldots, m$. If $|\varepsilon_{vil}| \geqslant 1, \forall l \in \{1, 2, \ldots, m\}$, we have $\gamma_2\sum_{i=1}^{N} p_i(\kappa_v\|\varepsilon_{vi}^{q_1}\|_1 + \rho_v\|\varepsilon_{vi}^{q_2}\|_1) \leqslant \gamma_2\sum_{i=1}^{N} p_i\ (\kappa_v|\varepsilon_{vi}|^{q_1} + \rho_v|\varepsilon_{vi}|^{q_2})^T|\varepsilon_{vi}| \leqslant (q_1 + 1)\gamma_2 V$.

If $|\varepsilon_{vil}| \leqslant 1, \forall l \in \{1, 2, \ldots, m\}, \gamma_2\sum_{i=1}^{N} p_i(\kappa_v\|\varepsilon_{vi}^{q_1}\|_1 + \rho_v\|\varepsilon_{vi}^{q_2}\|_1) \leqslant B_d$ holds for a positive constant $B_d$.

For a more general case, that is, if $|\varepsilon_{vil}| \leqslant 1$ holds just for some $l$. Then, we can get that $\gamma_2\sum_{i=1}^{N} p_i(\kappa_v\|\varepsilon_{vi}^{q_1}\|_1 + \rho_v\|\varepsilon_{vi}^{q_2}\|_1) \leqslant (q_1 + 1)\gamma_2 V + B_d$. Therefore, it can be obtained

$$\dot{V} \leqslant (q_1 + 1)\gamma_2 V + B_d. \tag{14}$$

By solving the above inequality, we can easily get

$$V \leqslant -\frac{B_d}{(q_1 + 1)\gamma_2} + (V(t_0) + \frac{B_d}{(q_1 + 1)\gamma_2})e^{(q_1+1)\gamma_2(t-t_0)}. \tag{15}$$

As a result, by inequality (15), the boundedness of $V$at any finite time interval $[t_0, t]$ can be obtained.

**Step 3**. In this step, we verify that the observation errors $\tilde{x}_{0i}$ and $\bar{\tilde{v}}_{0i}$ are able to converge to the origin within fixed time $T_0$. From Step 1, it follows that $\tilde{z}_x = \tilde{z}_v = 0, \forall t \geqslant T_1$. Then, for $t \geqslant T_1$, the dynamics of $\varepsilon_{xi}$ and $\varepsilon_{vi}$ reduce to

$$\begin{cases} \dot{\varepsilon}_{xi} = & \varepsilon_{vi} - \kappa_x(\sum_{j=1}^{N} a_{ij}(\lceil\varepsilon_{xi}\rfloor^{q_1} - \lceil\varepsilon_{xj}\rfloor^{q_1}) + b_i\lceil\varepsilon_{xi}\rfloor^{q_1}) \\ & -\rho_x(\sum_{j=1}^{N} a_{ij}(\lceil\varepsilon_{xi}\rfloor^{q_2} - \lceil\varepsilon_{xj}\rfloor^{q_2}) + b_i\lceil\varepsilon_{xi}\rfloor^{q_2}), \\ \dot{\varepsilon}_{vi} = & -\kappa_v(\sum_{j=1}^{N} a_{ij}(\lceil\varepsilon_{vi}\rfloor^{q_1} - \lceil\varepsilon_{vj}\rfloor^{q_1}) + b_i\lceil\varepsilon_{vi}\rfloor^{q_1}) \\ & -\rho_v(\sum_{j=1}^{N} a_{ij}(\lceil\varepsilon_{vi}\rfloor^{q_2} - \lceil\varepsilon_{vj}\rfloor^{q_2}) + b_i\lceil\varepsilon_{vi}\rfloor^{q_2}). \end{cases} \tag{16}$$

Firstly, consider the Lyapunov function candidate $V_2$. Its derivative with respect to time $t$ can be written as

$$\begin{aligned} \dot{V}_2 \leqslant\ & -\sum_{i=1}^{N} p_i(\kappa_v\lceil\varepsilon_{vi}\rfloor^{q_1} + \rho_v\lceil\varepsilon_{vi}\rfloor^{q_2})^T \times \\ & [\kappa_v(\sum_{j=1}^{N} a_{ij}(\lceil\varepsilon_{vi}\rfloor^{q_1} - \lceil\varepsilon_{vj}\rfloor^{q_1}) + b_i\lceil\varepsilon_{vi}\rfloor^{q_1})] \\ & -\sum_{i=1}^{N} p_i(\kappa_v\lceil\varepsilon_{vi}\rfloor^{q_1} + \rho_v\lceil\varepsilon_{vi}\rfloor^{q_2})^T \times \\ & [\rho_v(\sum_{j=1}^{N} a_{ij}(\lceil\varepsilon_{vi}\rfloor^{q_2} - \lceil\varepsilon_{vj}\rfloor^{q_2}) + \lceil\varepsilon_{vi}\rfloor^{q_2})] \\ =\ & -(\kappa_v\lceil\varepsilon_v\rfloor^{q_1} + \rho_v\lceil\varepsilon_v\rfloor^{q_2})^T PH \times \\ & (\kappa_v\lceil\varepsilon_v\rfloor^{q_1} + \rho_v\lceil\varepsilon_v\rfloor^{q_2}) \\ \leqslant\ & -\lambda_{\min}(Q)(\kappa_v^2\sum_{i=1}^{N} \varepsilon_{vi}^{q_1 T}\varepsilon_{vi}^{q_1} + 2\kappa_v\rho_v\sum_{i=1}^{N} \varepsilon_{vi}^{q_1 T}\varepsilon_{vi}^{q_2} \\ & +\rho_v^2\sum_{i=1}^{N} \varepsilon_{vi}^{q_2 T}\varepsilon_{vi}^{q_2}). \end{aligned} \tag{17}$$

Let $W_1 = \kappa_v^2\sum_{i=1}^{N} \varepsilon_{vi}^{q_1 T}\varepsilon_{vi}^{q_1} + 2\kappa_v\rho_v\sum_{i=1}^{N} \varepsilon_{vi}^{q_1 T}\varepsilon_{vi}^{q_2} + \rho_v^2 \times \sum_{i=1}^{N} \varepsilon_{vi}^{q_2 T}\varepsilon_{vi}^{q_2}$, we can get

$$\dot{V}_2 \leqslant -\lambda_{\min}(Q)W_1. \tag{18}$$

In addition, we define the following terms: $W_2 = V_2^{\frac{2q_1}{q_1+1}} = [\sum_{i=1}^{N}(p_i\frac{\kappa_v}{q_1+1}|\varepsilon_{vi}|^{q_1 T}|\varepsilon_{vi}| + p_i\frac{\rho_v}{q_2+1}|\varepsilon_{vi}|^{q_2 T}|\varepsilon_{vi}|)]^{\frac{2q_1}{q_1+1}}$ and $W_3 = V_2^{\frac{2q_2}{q_2+1}} = \left[\sum_{i=1}^{N}(p_i\frac{\kappa_v}{q_1+1}|\varepsilon_{vi}|^{q_1 T}|\varepsilon_{vi}| + p_i\frac{\rho_v}{q_2+1}|\varepsilon_{vi}|^{q_2 T} \times |\varepsilon_{vi}|)\right]^{\frac{2q_2}{q_2+1}}$.

By employing Lemmas 3 and 4 in [17], we have

$$\begin{aligned} W_2 \leqslant\ & 2^{\frac{q_1-1}{q_1+1}}\left(\sum_{i=1}^{N} p_i\frac{\kappa_v}{q_1+1}|\varepsilon_{vi}|^{q_1 T}|\varepsilon_{vi}|\right)^{\frac{2q_1}{q_1+1}} \\ & +2^{\frac{q_1-1}{q_1+1}}\left(\sum_{i=1}^{N} p_i\frac{\rho_v}{q_2+1}|\varepsilon_{vi}|^{q_2 T}|\varepsilon_{vi}|\right)^{\frac{2q_1}{q_1+1}} \\ \leqslant\ & 2^{\frac{q_1-1}{q_1+1}}[\left(p_M\frac{\kappa_v}{q_1+1}\right)^{\frac{2q_1}{q_1+1}}\left(\sum_{i=1}^{N}\|\varepsilon_{vi}\|_1\right)^{2q_1} \\ & +\left(p_M\frac{\rho_v}{q_2+1}\right)^{\frac{2q_1}{q_1+1}}\left(\sum_{i=1}^{N}\|\varepsilon_{vi}\|_1\right)^{\frac{2q_1(q_2+1)}{q_1+1}}], \end{aligned} \tag{19}$$

where $p_M = \max\{p_i\}, i = 1, 2, \ldots, N$.

$$\begin{aligned} W_3(\varepsilon_{vi}) \leqslant\ & \left(\sum_{i=1}^{N} p_i\frac{\kappa_v}{q_1+1}|\varepsilon_{vi}|^{q_1 T}|\varepsilon_{vi}|\right)^{\frac{2q_2}{q_2+1}} \\ & +\left(\sum_{i=1}^{N} p_i\frac{\rho_v}{q_2+1}|\varepsilon_{vi}|^{q_2 T}|\varepsilon_{vi}|\right)^{\frac{2q_2}{q_2+1}} \\ \leqslant\ & \left(p_M\frac{\kappa_v}{q_1+1}\right)^{\frac{2q_2}{q_2+1}}\left(\sum_{i=1}^{N}\|\varepsilon_{vi}\|_1\right)^{\frac{2q_2(q_1+1)}{q_2+1}} \\ & +\left(p_M\frac{\rho_v}{q_2+1}\right)^{\frac{2q_2}{q_2+1}}\left(\sum_{i=1}^{N}\|\varepsilon_{vi}\|_1\right)^{2q_2}. \end{aligned} \tag{20}$$

On behalf of verifying the fixed-time convergence of $\varepsilon_{vi}$, the following two cases need to be considered:

**Case 1**: If $0 < q_2 < \frac{1}{2}$, then $0 < 2q_2 < 1$. From Lemmas 3 and 4 in [17], we obtain

$$\begin{aligned} W_1(\varepsilon_{vi}) \geqslant\ & \kappa_v^2(Nm)^{1-2q_1}(\sum_{i=1}^{N}\|\varepsilon_{vi}\|_1)^{2q_1} \\ & +2\kappa_v\rho_v(Nm)^{1-q_1-q_2}(\sum_{i=1}^{N}\|\varepsilon_{vi}\|_1)^{q_1+q_2} \\ & +\rho_v^2(\sum_{i=1}^{N}\|\varepsilon_{vi}\|_1)^{2q_2}. \end{aligned} \tag{21}$$

If $\sum_{i=1}^{N}\|\varepsilon_{vi}\|_1 \leqslant 1$, on one hand, we have $W_1(\varepsilon_{vi}) \geqslant k_1(\sum_{i=1}^{N}\|\varepsilon_{vi}\|_1)^{2q_2}$ with $k_1 = \rho_v^2$; on the other hand, due to the fact $2q_1 \geqslant \frac{2q_1(2q_2+1)}{q_1+1} \geqslant 2q_2$ and $\frac{2q_2(2q_1+1)}{q_2+1} \geqslant 2q_2$, we get $(\sum_{i=1}^{N}\|\varepsilon_{vi}\|_1)^{2q_1} \leqslant (\sum_{i=1}^{N}\|\varepsilon_{vi}\|_1)^{2q_2}, (\sum_{i=1}^{N}\|\varepsilon_{vi}\|_1)^{\frac{2q_1(2q_2+1)}{q_1+1}} \leqslant (\sum_{i=1}^{N}\|\varepsilon_{vi}\|_1)^{2q_2}$, as well as $(\sum_{i=1}^{N}\|\varepsilon_{vi}\|_1)^{\frac{2q_2(2q_1+1)}{q_2+1}} \leqslant (\sum_{i=1}^{N}\|\varepsilon_{vi}\|_1)^{2q_2}$.

Thus, we can obtain

$$\begin{aligned} \dot{V}_2 \leqslant\ & -k_1\left(\sum_{i=1}^{N}\|\varepsilon_{vi}\|_1\right)^{2q_2} \\ \leqslant\ & -\Delta_1\left[(V_2)^{\frac{2q_1}{q_1+1}} + (V_2)^{\frac{2q_2}{q_2+1}}\right], \end{aligned} \tag{22}$$

where $\Delta_1 = \frac{k_1}{\Omega}$ with $\Omega = \left(p_M\frac{\kappa_v}{q_1+1}\right)^{\frac{2q_2}{q_2+1}} + \left(p_M\frac{\rho_v}{q_2+1}\right)^{\frac{2q_2}{q_2+1}} + 2^{\frac{q_1-1}{q_1+1}}\left(p_M\frac{\kappa_v}{q_1+1}\right)^{\frac{2q_1}{q_1+1}} + 2^{\frac{q_1-1}{q_1+1}}\left(p_M\frac{\rho_v}{q_2+1}\right)^{\frac{2q_1}{q_1+1}}$.

If $\sum_{i=1}^{N}\|\varepsilon_{vi}\|_1 > 1$, on one hand, we have $W_1(\varepsilon_{vi}) \geqslant \bar{k}_1(\sum_{i=1}^{N}\|\varepsilon_{vi}\|_1)^{2q_1}$ with $\bar{k}_1 = \kappa_v^2(Nm)^{1-2q_1}$; on the other hand, due to the fact $2q_1 \geqslant \frac{2q_1(2q_2+1)}{q_1+1} \geqslant 2q_2$ and $2q_1 \geqslant \frac{2q_2(2q_1+1)}{q_2+1}$, we get $(\sum_{i=1}^{N}\|\varepsilon_{vi}\|_1)^{2q_2} \leqslant (\sum_{i=1}^{N}\|\varepsilon_{vi}\|_1)^{2q_1}, (\sum_{i=1}^{N}\|\varepsilon_{vi}\|_1)^{\frac{2q_1(2q_2+1)}{q_1+1}} \leqslant (\sum_{i=1}^{N}\|\varepsilon_{vi}\|_1)^{2q_1}$, and $(\sum_{i=1}^{N}\|\varepsilon_{vi}\|_1)^{\frac{2q_2(2q_1+1)}{q_2+1}} \leqslant (\sum_{i=1}^{N}\|\varepsilon_{vi}\|_1)^{2q_1}$.

Similarly, we get

$$\begin{aligned} \dot{V}_2 \leqslant & -\bar{k}_1\left(\sum_{i=1}^{N}\|\varepsilon_{vi}\|_1\right)^{2q_2} \\ \leqslant & -\bar{\Delta}_1\left[(V_2)^{\frac{2q_1}{q_1+1}} + (V_2)^{\frac{2q_2}{q_2+1}}\right], \end{aligned} \tag{23}$$

where $\bar{\Delta}_1 = \frac{\bar{k}_1}{\Omega}$.

**Case 2**: If $\frac{1}{2} \leqslant q_2 < 1$, then $2q_2 \geqslant 1$. According to Lemmas 3 and 4 in [17], we obtain

$$\begin{aligned} W_1(\varepsilon_{vi}) \geqslant & \kappa_v^2(Nm)^{1-2q_1}(\sum_{i=1}^{N}\|\varepsilon_{vi}\|_1)^{2q_1} \\ & +\rho_v^2(Nm)^{1-2q_2}(\sum_{i=1}^{N}\|\varepsilon_{vi}\|_1)^{2q_2} \\ & +2\kappa_v\rho_v(Nm)^{1-q_1-q_2}(\sum_{i=1}^{N}\|\varepsilon_{vi}\|_1)^{q_1+q_2}. \end{aligned} \tag{24}$$

If $\sum_{i=1}^{N}\|\varepsilon_{vi}\|_1 \leqslant 1$, on one hand, we get $W_1(\varepsilon_{vi}) \geqslant k_2(\sum_{i=1}^{N}\|\varepsilon_{vi}\|_1)^{2q_2}$ with $k_2 = \rho_v^2(Nm)^{1-2q_2}$; on the other hand, it can be easily obtained that $(\sum_{i=1}^{N}\|\varepsilon_{vi}\|_1)^{2q_1} \leqslant (\sum_{i=1}^{N}\|\varepsilon_{vi}\|_1)^{2q_2}, (\sum_{i=1}^{N}\|\varepsilon_{vi}\|_1)^{\frac{2q_1(2q_2+1)}{q_1+1}} \leqslant (\sum_{i=1}^{N}\|\varepsilon_{vi}\|_1)^{2q_2}$, and $(\sum_{i=1}^{N}\|\varepsilon_{vi}\|_1)^{\frac{2q_2(2q_1+1)}{q_2+1}} \leqslant (\sum_{i=1}^{N}\|\varepsilon_{vi}\|_1)^{2q_2}$.

Thus, we can obtain

$$\begin{aligned} \dot{V}_2 \leqslant & -k_2\left(\sum_{i=1}^{N}\|\varepsilon_{vi}\|_1\right)^{2q_2} \\ \leqslant & -\Delta_2\left[(V_2)^{\frac{2q_1}{q_1+1}} + (V_2)^{\frac{2q_2}{q_2+1}}\right], \end{aligned} \tag{25}$$

where $\Delta_2 = \frac{k_2}{\Omega}$.

If $\sum_{i=1}^{N}\|\varepsilon_{vi}\|_1 > 1$, on one hand, we can get $W_1(\varepsilon_{vi}) \geqslant \bar{k}_2(\sum_{i=1}^{N}\|\varepsilon_{vi}\|_1)^{2q_1}$ with $\bar{k}_2 = \bar{k}_1$; on the other hand, we have $(\sum_{i=1}^{N}\|\varepsilon_{vi}\|_1)^{2q_2} \leqslant (\sum_{i=1}^{N}\|\varepsilon_{vi}\|_1)^{2q_1}, (\sum_{i=1}^{N}\|\varepsilon_{vi}\|_1)^{\frac{2q_2(2q_1+1)}{q_2+1}} \leqslant (\sum_{i=1}^{N}\|\varepsilon_{vi}\|_1)^{2q_1}$, as well as $(\sum_{i=1}^{N}\|\varepsilon_{vi}\|_1)^{\frac{2q_1(2q_2+1)}{q_1+1}} \leqslant (\sum_{i=1}^{N}\|\varepsilon_{vi}\|_1)^{2q_1}$.

Similarly, we get

$$\begin{aligned} \dot{V}_2 \leqslant & -\bar{k}_2\left(\sum_{i=1}^{N}\|\varepsilon_{vi}\|_1\right)^{2q_2} \\ \leqslant & -\bar{\Delta}_2\left[(V_2)^{\frac{2q_1}{q_1+1}} + (V_2)^{\frac{2q_2}{q_2+1}}\right], \end{aligned} \tag{26}$$

where $\bar{\Delta}_2 = \frac{\bar{k}_2}{\Omega}$.

Combining the above cases, we can obtain

$$\dot{V}_2 \leqslant -\Delta\left[(V_2)^{\frac{2q_1}{q_1+1}} + (V_2)^{\frac{2q_2}{q_2+1}}\right], \tag{27}$$

where

$$\Delta = \begin{cases} \min\{\Delta_1, \bar{\Delta}_1\}, & \text{if } 0 \leqslant q_2 < \frac{1}{2}; \\ \min\{\Delta_2, \bar{\Delta}_2\}, & rmif\ \frac{1}{2} \leqslant q_2 < 1. \end{cases} \tag{28}$$

Therefore, from Lemma 2 in [17] and inequality Eqn 27, we can conclude that $\varepsilon_{vi}$ will converge to the origin within fixed time $T_2$, which is bounded by

$$T_2 \leqslant \frac{(q_1+1)}{\Delta(q_1-1)} + \frac{(q_2+1)}{\Delta(1-q_2)}. \tag{29}$$

After the convergence of $\varepsilon_{vi}$, the dynamics of $\varepsilon_{xi}$ can be rewritten as

$$\begin{aligned} \dot{\varepsilon}_{xi} = & -\kappa_x(\sum_{j=1}^{N} a_{ij}(\lceil\varepsilon_{xi}\rfloor^{q_1} - \lceil\varepsilon_{xj}\rfloor^{q_1}) + b_i\lceil\varepsilon_{xi}\rfloor^{q_1}) \\ & -\rho_x(\sum_{j=1}^{N} a_{ij}(\lceil\varepsilon_{xi}\rfloor^{q_2} - \lceil\varepsilon_{xj}\rfloor^{q_2}) + b_i\lceil\varepsilon_{xi}\rfloor^{q_2}). \end{aligned} \tag{30}$$

Similarly, we obtain that the $\varepsilon_{xi}$ can converge to the origin within $T_3$ after the convergence of $\varepsilon_{vi}$, which is bounded by

$$T_3 \leqslant \frac{(q_1+1)}{\tilde{\Delta}(q_1-1)} + \frac{(q_2+1)}{\tilde{\Delta}(1-q_2)}. \tag{31}$$

In this inequality,

$$\tilde{\Delta} = \begin{cases} \min\{\Delta_3, \bar{\Delta}_3\}, & \text{if } \frac{1}{2} \leqslant q_2 < \frac{1}{2}; \\ \min\{\Delta_4, \bar{\Delta}_4\}, & \text{if } \frac{1}{2} \leqslant q_2 < 1, \end{cases} \tag{32}$$

where $\Delta_3 = \frac{k_3}{\tilde{\Omega}}, \bar{\Delta}_3 = \frac{\bar{k}_3}{\tilde{\Omega}}, \Delta_4 = \frac{k_4}{\tilde{\Omega}}$ and $\bar{\Delta}_4 = \frac{\bar{k}_4}{\tilde{\Omega}}$ with $\tilde{\Omega} = \left(p_M\frac{\kappa_x}{q_1+1}\right)^{\frac{2q_2}{q_2+1}} + \left(p_M\frac{\rho_x}{q_2+1}\right)^{\frac{2q_2}{q_2+1}} + 2^{\frac{q_1-1}{q_1+1}}\left(p_M\frac{\kappa_x}{q_1+1}\right)^{\frac{2q_1}{q_1+1}} + 2^{\frac{q_1-1}{q_1+1}}\left(p_M\frac{\rho_x}{q_2+1}\right)^{\frac{2q_1}{q_1+1}}, k_3 = \rho_x^2, \bar{k}_3 = \kappa_x^2(Nm)^{1-2q_1}, k_4 = \rho_x^2(mN)^{1-2q_2}$, and $\bar{k}_4 = \bar{k}_3$.

Thus, from the above analysis, it can be proved that $\varepsilon_x$ and $\varepsilon_v$ will converge to the origin in fixed time $T_0 = T_1 + T_2 + T_3$. From Lemma 1 in [9], matrix $H$ is invertible. Then, $\eta_x$ and $\eta_v$ can converge to the origin within fixed time $T_0$ due to $\varepsilon_x = H\eta_x$ and $\varepsilon_v = H\eta_v$. Furthermore, due to $z_v = v_0$ when $t \geqslant T_1$, the observation errors $\tilde{x}_0$ and $\bar{\tilde{v}}_0$ will converge to the origin in fixed time $T_0$.

As a result, the proposed CFTSO can provide the estimates of the LSs $x_0$ and $v_0$ for each follower under directed topologies without the LVMs within fixed time $T_0$. This completes the proof.

### *3.2. Radial basis function neural network and minimal learning parameter technique*

It is assumed that the uncertain term $f_i(x_i, v_i) \in R^m$ can be described on a prescribed compact set $\Pi \in R^{2m}$ by

$$f_i(x_i, v_i) = \omega_i^T\phi_i(x_i, v_i)1_m + \varepsilon_i, \tag{33}$$

where $\phi_i = \mathrm{diag}(\phi_{i,1}, \phi_{i,2}, \ldots, \phi_{i,m}) \in R^{m\zeta_i \times m}$ with $\phi_{i,l} = [\phi_{i,l,1}^T, \phi_{i,l,2}^T, \ldots, \phi_{i,l,\zeta_i}^T]^T \in R^{\zeta_i}$ being a set of $\zeta_i$ Gaussian functions with $l = 1, 2, \ldots, m$. $\omega_i = \mathrm{diag}(\omega_{i,1}, \omega_{i,2}, \ldots, \omega_{i,m}) \in R^{m\zeta_i \times m}$ is the ideal RBFNN weight matrix with $\omega_{i,l} \in R^{\zeta_i}$, and $\varepsilon_i$ is the RBFNN approximation error vector. In real applications, the approximation of $f_i$ can be given by

$$\hat{f}_i(x_i, v_i) = \hat{\omega}_i^T\phi_i(x_i, v_i)1_m, \tag{34}$$

where $\hat{\omega}_i = \mathrm{diag}(\hat{\omega}_{i,1}, \hat{\omega}_{i,2}, \ldots, \hat{\omega}_{i,m}) \in R^{m\zeta_i \times m}$ with $\hat{\omega}_{i,l} \in R^{\zeta_i}$ is the current estimate vector of the RBFNN weight for the $i$th follower.

In addition, we define the error matrix of the RBFNN weights as $\tilde{\omega}_i = \omega_i - \hat{\omega}_i$.

**Remark 4.** According to Stone-Weierstrass approximation theorem, there exist positive constants $\phi_M, W_M, \varepsilon_M$, such that $\|\phi_i\|_F \leqslant \phi_M, \|w_i\|_F \leqslant W_M$ and $\|\varepsilon_i\|_2 \leqslant \varepsilon_M$.

To reduce the computation burden, in this paper, MLP technique is employed. Define $\theta_i = \mathrm{diag}\{\theta_{i,1}, \theta_{i,2}, \ldots, \theta_{i,m}\}$ with $\theta_{i,l} = \|\omega_{i,l}\|_2^2, l = 1, 2, \ldots, m$. Let $\hat{\theta}_i = \mathrm{diag}\{\hat{\theta}_{i,1}, \hat{\theta}_{i,2}, \ldots, \hat{\theta}_{i,m}\}$, where $\hat{\theta}_{i,l}$ is the approximation of $\theta_{i,l}$. Therefore, the weight vector $\hat{\omega}_{i,l}$ is converted to its norm parameter $\hat{\theta}_{i,l}$, which can decrease the number of the adaptive parameters significantly. Then, according to Remark 4, $\|\theta_i\|_F \leqslant \theta_M$ holds for a positive constant $\theta_M$.

### 3.3. Fixed-time time-varying formation control scheme design and analysis

Firstly, the formation tracking control law will be proposed by adopting backstepping method. Then, the fixed-time stability of the closed-loop MAS with uncertainties will be given.

For the $i$th follower, define the auxiliary formation tracking position and velocity error vectors $e_{xi}$ and $e_{vi}$ as

$$\begin{cases} e_{xi} = x_i - h_{xi} - \hat{x}_{0i} = x_i - h_{xi} - \tilde{x}_{0i} - x_0, \\ e_{vi} = v_i - h_{vi} - \hat{v}_{0i} = v_i - h_{vi} - \tilde{v}_{0i} - v_0 - \tilde{z}_v. \end{cases} \tag{35}$$

Substituting (5) and (7) into (35), the dynamics of $e_{xi}$ and $e_{vi}$ for the $i$th follower is

$$\begin{cases} \dot{e}_{xi} = & e_{vi} - \kappa_x \lceil \sum_{j=1}^N a_{ij}(\tilde{x}_{0j} - \tilde{x}_{0i}) - b_i \tilde{x}_{0i} \rfloor^{q_1} \\ & -\rho_x \lceil \sum_{j=1}^N a_{ij}(\tilde{x}_{0j} - \tilde{x}_{0i}) - b_i \tilde{x}_{0i} \rfloor^{q_2} + \tilde{z}_v, \\ \dot{e}_{vi} = & -\kappa_v \lceil \sum_{j=1}^N a_{ij}(\hat{v}_{0j} - \hat{v}_{0i}) + b_i(z_v - \hat{v}_{0i}) \rfloor^{q_1} \\ & -\rho_v \lceil \sum_{j=1}^N a_{ij}(\hat{v}_{0j} - \hat{v}_{0i}) + b_i(z_v - \hat{v}_{0i}) \rfloor^{q_2} \\ & + f_i + u_i - \dot{h}_{vi} - b_i u_0, i = 1, 2, \ldots, N. \end{cases} \tag{36}$$

Firstly, choose $e_{vi}$ as the virtual control input. The virtual control law $\sigma_i$ is designed as

$$\sigma_i = -\lambda_1 \lceil e_{xi} \rfloor^{\mu_1} - \lambda_2 \lceil e_{xi} \rfloor^{\mu_2}, \tag{37}$$

where $\lambda_1, \lambda_2 > 0, \mu_1 > 1, 0 < \mu_2 < 1$.

Select a Lyapunov candidate function as

$$V_3 = \frac{1}{2} e_{xi}^T e_{xi}. \tag{38}$$

The time differentiation of (38) is deduced as follows

$$\begin{aligned} \dot{V}_3 = \; & e_{xi}^T (-\lambda_1 \lceil e_{xi} \rfloor^{\mu_1} - \lambda_2 \lceil e_{xi} \rfloor^{\mu_2} \\ & -\kappa_x \lceil \sum_{j=1}^N a_{ij}(\tilde{x}_{0j} - \tilde{x}_{0i}) - b_i \tilde{x}_{0i} \rfloor^{q_1} \\ & -\rho_x \lceil \sum_{j=1}^N a_{ij}(\tilde{x}_{0j} - \tilde{x}_{0i}) - b_i \tilde{x}_{0i} \rfloor^{q_2} + \tilde{z}_v). \end{aligned} \tag{39}$$

According to Theorem 1, both $\varepsilon_{xi}$ and $\tilde{z}_v$ are always bounded. Therefore, through adopting Young's inequality, there exists a constant $\varrho_1 > 0$ so that the following inequality holds

$$\begin{aligned} & e_{xi}^T (-\kappa_x \lceil \sum_{j=1}^N a_{ij}(\tilde{x}_{0j} - \tilde{x}_{0i}) - b_i \tilde{x}_{0i} \rfloor^{q_1} \\ & -\rho_x \lceil \sum_{j=1}^N a_{ij}(\tilde{x}_{0j} - \tilde{x}_{0i}) - b_i \tilde{x}_{0i} \rfloor^{q_2} + \tilde{z}_v) \\ & \leqslant \tfrac{1}{2} e_{xi}^T e_{xi} + \varrho_1. \end{aligned} \tag{40}$$

Utilizing Lemmas 3 and 4 in [17], and on the basis of the fact that $V_3 \leqslant V_3^{\frac{\mu_1+1}{2}} + V_3^{\frac{\mu_2+1}{2}}, \dot{V}_3$ turns into

$$\begin{aligned} \dot{V}_3 \leqslant \; & -2^{\frac{\mu_1+1}{2}} m^{\frac{1-\mu_1}{2}} \lambda_1 V_3^{\frac{\mu_1+1}{2}} - 2^{\frac{\mu_2+1}{2}} \lambda_2 V_3^{\frac{\mu_2+1}{2}} \\ & + V_3 + \varrho_1 \\ \leqslant \; & -(2^{\frac{\mu_1+1}{2}} m^{\frac{1-\mu_1}{2}} \lambda_1 - 1) V_3^{\frac{\mu_1+1}{2}} \\ & -(2^{\frac{\mu_2+1}{2}} \lambda_2 - 1) V_3^{\frac{\mu_2+1}{2}} + \varrho_1. \end{aligned} \tag{41}$$

According to the above inequality and Lemma 2.2 in [27], $e_{xi}$ will converge to a small neighborhood of the origin within a fixed time if the following two conditions that $2^{\frac{\mu_1+1}{2}} m^{\frac{1-\mu_1}{2}} \lambda_1 - 1 > 0$ and $2^{\frac{\mu_2+1}{2}} \lambda_2 - 1 > 0$ are satisfied.

Then, the following nonlinear nonsmooth filter is introduced to deal with the explosion of complexity problem:

$$\tau_i \dot{\sigma}_{di} = \lceil \sigma_i - \sigma_{di} \rfloor^{\mu_1} + \lceil \sigma_i - \sigma_{di} \rfloor^{\mu_2}, \sigma_{di}(t_0) = \sigma_i(t_0), \tag{42}$$

where $\tau_i$ is a small positive constant and the state $\sigma_{id}$ is the output of the filter.

Define the tracking error as $\bar{e}_{vi} = e_{vi} - \sigma_{di}$. The dynamics of $e_{xi}$ and $\bar{e}_{vi}$ are written as

$$\begin{cases} \dot{e}_{xi} = & \bar{e}_{vi} + \sigma_{id} - \kappa_x \lceil \sum_{j=1}^N a_{ij}(\tilde{x}_{0j} - \tilde{x}_{0i}) - b_i \tilde{x}_{0i} \rfloor^{q_1} \\ & -\rho_x \lceil \sum_{j=1}^N a_{ij}(\tilde{x}_{0j} - \tilde{x}_{0i}) - b_i \tilde{x}_{0i} \rfloor^{q_2} + \tilde{z}_v, \\ \dot{\bar{e}}_{vi} = & -\kappa_v \lceil \sum_{j=1}^N a_{ij}(\hat{v}_{0j} - \hat{v}_{0i}) + b_i(z_v - \hat{v}_{0i}) \rfloor^{q_1} \\ & -\rho_v \lceil \sum_{j=1}^N a_{ij}(\hat{v}_{0j} - \hat{v}_{0i}) + b_i(z_v - \hat{v}_{0i}) \rfloor^{q_2} \\ & + f_i + u_i - \dot{h}_{vi} - \dot{\sigma}_{id} - b_i u_0, i = 1, 2, \ldots, N. \end{cases} \tag{43}$$

Thus, the actual control law $u_i$ for the $i$th follower can be designed as

$$\begin{aligned} u_i = \; & -\gamma_1 \lceil \bar{e}_{vi} \rfloor^{\mu_1} - \gamma_2 \lceil \bar{e}_{vi} \rfloor^{\mu_2} + \dot{h}_{vi} \\ & -\tfrac{1}{2} \hat{\theta}_i^T \phi_i^T \phi_i \bar{e}_{vi} + b_i u_0 + \dot{\sigma}_{di}, \end{aligned} \tag{44}$$

where $\gamma_1, \gamma_2 > 0$, and $\dot{\sigma}_{id}$ is acquired through (42).

The corresponding adaptive law is designed as

$$\dot{\hat{\theta}}_i = \frac{1}{2} \psi_i \phi_i^T \phi_i E_{vi} - \vartheta_i \hat{\theta}_i \psi_i, \; i = 1, 2, \ldots, N, \tag{45}$$

where constants $\psi_i, \vartheta_i > 0$, and $E_{vi}$ is a diagonal matrix with the elements of its principal diagonal being the same as the corresponding ones of the matrix $\bar{e}_{vi} \bar{e}_{vi}^T$.

Define the filtering error of the nonsmooth filter (42) as

$$\tilde{\sigma}_i = \sigma_i - \sigma_{di}. \tag{46}$$

The time differentiation of (46) yields that

$$\dot{\tilde{\sigma}}_i = -(\lceil \tilde{\sigma}_i \rfloor^{\mu_1} + \lceil \tilde{\sigma}_i \rfloor^{\mu_2}) / \tau_i + \dot{\sigma}_i. \tag{47}$$

Construct the following Lyapunov function

$$V_4 = V_3 + \frac{1}{2} \bar{e}_{vi}^T \bar{e}_{vi} + \frac{1}{2} \mathrm{tr}(\tilde{\theta}_i^T \psi_i^{-1} \tilde{\theta}_i) + \frac{1}{2} \tilde{\sigma}_i^T \tilde{\sigma}_i. \tag{48}$$

Then, the derivative of $V_4$ with respect to time is

$$
\begin{aligned}
\dot{V}_4 = \quad & e_{xi}^T(-\lambda_1\lceil e_{xi}\rfloor^{\mu_1} - \lambda_2\lceil e_{xi}\rfloor^{\mu_2} + \tilde{z}_v \\
& -\kappa_x\lceil\sum_{j=1}^N a_{ij}(\tilde{x}_{0j} - \tilde{x}_{0i}) - b_i\tilde{x}_{0i}\rfloor^{q_1} + \bar{e}_{vi} \\
& -\rho_x\lceil\sum_{j=1}^N a_{ij}(\tilde{x}_{0j} - \tilde{x}_{0i}) - b_i\tilde{x}_{0i}\rfloor^{q_2} - \tilde{\sigma}_i) \\
& +\bar{e}_{vi}^T(-\gamma_1\lceil\bar{e}_{vi}\rfloor^{\mu_1} - \gamma_2\lceil\bar{e}_{vi}\rfloor^{\mu_2} \\
& -\tfrac{1}{2}\hat{\theta}_i^T\phi_i^T\phi_i\bar{e}_{vi} + \omega_i^T\phi_i 1_m + \varepsilon_i \\
& -\kappa_v\lceil\sum_{j=1}^N a_{ij}(\hat{v}_{0j} - \hat{v}_{0i}) + b_i(z_v - \hat{v}_{0i})\rfloor^{q_1} \\
& -\rho_v\lceil\sum_{j=1}^N a_{ij}(\hat{v}_{0j} - \hat{v}_{0i}) + b_i(z_v - \hat{v}_{0i})\rfloor^{q_2}) \\
& +\mathrm{tr}(\dot{\tilde{\theta}}_i\psi_i\tilde{\theta}_i) + \tilde{\sigma}_i^T\dot{\tilde{\sigma}}_i, i = 1,2,\ldots,N.
\end{aligned} \tag{49}
$$

By applying Young's inequality, it is easy to deduce that $\bar{e}_{vi}^T\omega_i^T\phi_i 1_m \leqslant \frac{1}{2}\bar{e}_{vi}^T\theta_i\phi_i^T\phi_i\bar{e}_{vi} + \frac{m}{2}$. Let $\tilde{\theta}_i = \theta_i - \hat{\theta}_i$. Substituting the adaptive law (45) into (49) and invoking $y_1^Ty_2 = \mathrm{tr}(y_2y_1^T)$, $\forall y_1, y_2 \in R^n$, we can further get

$$
\begin{aligned}
\dot{V}_4 = \quad & e_{xi}^T(-\lambda_1\lceil e_{xi}\rfloor^{\mu_1} - \lambda_2\lceil e_{xi}\rfloor^{\mu_2} + \tilde{z}_v \\
& -\kappa_x\lceil\sum_{j=1}^N a_{ij}(\tilde{x}_{0j} - \tilde{x}_{0i}) - b_i\tilde{x}_{0i}\rfloor^{q_1} + \bar{e}_{vi} \\
& -\rho_x\lceil\sum_{j=1}^N a_{ij}(\tilde{x}_{0j} - \tilde{x}_{0i}) - b_i\tilde{x}_{0i}\rfloor^{q_2} - \tilde{\sigma}_i) \\
& +\vartheta_i\mathrm{tr}(\theta_i^T\tilde{\theta}_i) - \vartheta_i\mathrm{tr}(\tilde{\theta}_i^T\tilde{\theta}_i) \\
& +\bar{e}_{vi}^T(-\gamma_1\lceil\bar{e}_{vi}\rfloor^{\mu_1} - \gamma_2\lceil\bar{e}_{vi}\rfloor^{\mu_2} + \varepsilon_i \\
& -\kappa_v\lceil\sum_{j=1}^N a_{ij}(\hat{v}_{0j} - \hat{v}_{0i}) + b_i(z_v - \hat{v}_{0i})\rfloor^{q_1} \\
& -\rho_v\lceil\sum_{j=1}^N a_{ij}(\hat{v}_{0j} - \hat{v}_{0i}) + b_i(z_v - \hat{v}_{0i})\rfloor^{q_2} \\
& -\tilde{\sigma}_i^T(\lceil\tilde{\sigma}_i\rfloor^{\mu_1} + \lceil\tilde{\sigma}_i\rfloor^{\mu_2})/\tau_i + \tilde{\sigma}_i^T\dot{\sigma}_i, i = 1,2,\ldots,N.
\end{aligned} \tag{50}
$$

**Theorem 2.** *Consider the MASs constructed by N followers and one leader. Suppose Assumptions 1 and 2 hold. Then, under the control law (44) and the adaptive law (45), the MASs can realize the desired time-varying formation within a fixed time, if the following condition is satisfied*

$$
\begin{cases}
2^{\frac{\mu_1+1}{2}}m^{\frac{1-\mu_1}{2}}\lambda_1 - 3 > 0, \\
2^{\frac{\mu_2+1}{2}}\lambda_2 - 3 > 0, \\
2^{\frac{\mu_1+1}{2}}m^{\frac{1-\mu_1}{2}}\gamma_1 - 2 > 0, \\
2^{\frac{\mu_2+1}{2}}\gamma_2 - 2 > 0, \\
\frac{1}{\tau_i}2^{\frac{\mu_1+1}{2}}m^{\frac{1-\mu_1}{2}} - 2 > 0, \\
\frac{1}{\tau_i}2^{\frac{\mu_2+1}{2}} - 2 > 0.
\end{cases} \tag{51}
$$

**Proof 2.** The proof consists of two steps. Firstly, we verify that $e_{xi}, \bar{e}_{vi}, \tilde{\theta}_i$ and $\tilde{\sigma}_i$ are UUB. Secondly, we prove that $e_{xi}, \bar{e}_{vi}$ and $\tilde{\sigma}_i$ are able to converge to a small region around the origin within a fixed time.

**Step 1.** From Theorem 1, $\tilde{x}_{0i}, \tilde{z}_v$ and $\varepsilon_{vi}$ are all bounded. Thus, we can get

$$
\begin{aligned}
& e_{xi}^T(-\kappa_x\lceil\sum_{j=1}^N a_{ij}(\tilde{x}_{0j} - \tilde{x}_{0i}) - b_i\tilde{x}_{0i}\rfloor^{q_1}) \\
& +e_{xi}^T(-\rho_x\lceil\sum_{j=1}^N a_{ij}(\tilde{x}_{0j} - \tilde{x}_{0i}) - b_i\tilde{x}_{0i}\rfloor^{q_2} + \tilde{z}_v)) \\
& +\bar{e}_{vi}^T(-\kappa_v\lceil\sum_{j=1}^N a_{ij}(\hat{v}_{0j} - \hat{v}_{0i}) + b_i(z_v - \hat{v}_{0i})\rfloor^{q_1} \\
& +\bar{e}_{vi}^T(-\rho_v\lceil\sum_{j=1}^N a_{ij}(\hat{v}_{0j} - \hat{v}_{0i}) + b_i(z_v - \hat{v}_{0i})\rfloor^{q_2}) \\
& \quad \leqslant \tfrac{1}{2}e_{xi}^Te_{xi} + \tfrac{1}{2}\bar{e}_{vi}^T\bar{e}_{vi} + \varrho_2,
\end{aligned} \tag{52}
$$

where $\varrho_2$ is a positive constant. In addition, by invoking Young's inequality, we have $e_{xi}^T(\bar{e}_{vi} - \tilde{\sigma}_i) \leqslant e_{xi}^Te_{xi} + \frac{1}{2}\bar{e}_{vi}^T\bar{e}_{vi} + \frac{1}{2}\tilde{\sigma}_i^T\tilde{\sigma}_i$. Therefore, (50) can be rewritten as

$$
\begin{aligned}
\dot{V}_4 \leqslant \quad & e_{xi}^T(-\lambda_1\lceil e_{xi}\rfloor^{\mu_1} - \lambda_2\lceil e_{xi}\rfloor^{\mu_2}) + \tfrac{3}{2}e_{xi}^Te_{xi} \\
& +\bar{e}_{vi}^T(-\gamma_1\lceil\bar{e}_{vi}\rfloor^{\mu_1} - \gamma_2\lceil\bar{e}_{vi}\rfloor^{\mu_2} + \varepsilon_i) + \bar{e}_{vi}^T\bar{e}_{vi} \\
& -\vartheta_i\mathrm{tr}(\tilde{\theta}_i^T\tilde{\theta}_i) - \tilde{\sigma}_i^T(\lceil\tilde{\sigma}_i\rfloor^{\mu_1} + \lceil\tilde{\sigma}_i\rfloor^{\mu_2})/\tau_i \\
& +\tfrac{1}{2}\tilde{\sigma}_i^T\tilde{\sigma}_i + \tilde{\sigma}_i^T\dot{\sigma}_i + \vartheta_i\mathrm{tr}(\theta_i^T\tilde{\theta}_i) + \varrho_2.
\end{aligned} \tag{53}
$$

Similar to [35–37], it is supposed that $\|\dot{\sigma}_i\|_2^2 \leqslant \sigma_{Mi}$ holds a positive constant $\sigma_{Mi}$. Thus, by utilizing Young's inequality, we can get that

$$
\tilde{\sigma}_i^T\dot{\sigma}_i \leqslant \frac{1}{2}\tilde{\sigma}_i^T\tilde{\sigma}_i + \frac{1}{2}\sigma_{Mi}. \tag{54}
$$

Furthermore, by utilizing Lemmas 3–4, if condition (51) holds, we can obtain that

$$
\begin{aligned}
\dot{V}_4 \leqslant \quad & e_{xi}^T(-\lambda_1\lceil e_{xi}\rfloor^{\mu_1} - \lambda_2\lceil e_{xi}\rfloor^{\mu_2}) + \tfrac{3}{2}e_{xi}^Te_{xi} \\
& +\bar{e}_{vi}^T(-\gamma_1\lceil\bar{e}_{vi}\rfloor^{\mu_1} - \gamma_2\lceil\bar{e}_{vi}\rfloor^{\mu_2} + \varepsilon_i) + \bar{e}_{vi}^T\bar{e}_{vi} \\
& -\vartheta_i\mathrm{tr}(\tilde{\theta}_i^T\tilde{\theta}_i) - \tilde{\sigma}_i^T(\lceil\tilde{\sigma}_i\rfloor^{\mu_1} + \lceil\tilde{\sigma}_i\rfloor^{\mu_2})/\tau_i \\
& +\tilde{\sigma}_i^T\tilde{\sigma}_i + \vartheta_i\mathrm{tr}(\theta_i^T\tilde{\theta}_i) + \varrho_2 + \tfrac{1}{2}\sigma_{Mi} \\
\leqslant \quad & -(2^{\frac{\mu_1+1}{2}}m^{\frac{1-\mu_1}{2}}\lambda_1 - 3)(\tfrac{1}{2}e_{xi}^Te_{xi})^{\frac{\mu_1+1}{2}} \\
& -(2^{\frac{\mu_2+1}{2}}\lambda_2 - 3)(\tfrac{1}{2}e_{xi}^Te_{xi})^{\frac{\mu_2+1}{2}} \\
& -(2^{\frac{\mu_1+1}{2}}m^{\frac{1-\mu_1}{2}}\gamma_1 - 2)(\tfrac{1}{2}\bar{e}_{vi}^T\bar{e}_{vi})^{\frac{\mu_1+1}{2}} \\
& -(2^{\frac{\mu_2+1}{2}}\gamma_2 - 2)(\tfrac{1}{2}\bar{e}_{vi}^T\bar{e}_{vi})^{\frac{\mu_2+1}{2}} \\
& -(\tfrac{1}{\tau_i}2^{\frac{\mu_1+1}{2}}m^{\frac{1-\mu_1}{2}} - 2)(\tfrac{1}{2}\tilde{\sigma}_i^T\tilde{\sigma}_i)^{\frac{\mu_1+1}{2}} \\
& -(\tfrac{1}{\tau_i}2^{\frac{\mu_2+1}{2}} - 2)(\tfrac{1}{2}\tilde{\sigma}_i^T\tilde{\sigma}_i)^{\frac{\mu_2+1}{2}} \\
& -\tfrac{1}{2}\vartheta_i\mathrm{tr}(\tilde{\theta}_i^T\tilde{\theta}_i) + Q_1 \\
\leqslant \quad & -\tfrac{1}{2}\xi_1(e_{xi}^Te_{xi} + \bar{e}_{vi}^T\bar{e}_{vi} + \tilde{\sigma}_i^T\tilde{\sigma}_i \\
& +\mathrm{tr}(\tilde{\theta}_i^T\psi_i^{-1}\tilde{\theta}_i)) + Q_1 \\
= \quad & -\xi_1 V_4 + Q_1,
\end{aligned} \tag{55}
$$

where positive number $Q_1 = \varrho_2 + \frac{1}{2}\sigma_{Mi} + \frac{1}{2}\vartheta_i\theta_M^2 + \frac{1}{2}\varepsilon_M^2$, and $\xi_1 = \min\{2^{\frac{\mu_1+1}{2}}m^{\frac{1-\mu_1}{2}}\lambda_1 - 3, 2^{\frac{\mu_2+1}{2}}\lambda_2 - 3, 2^{\frac{\mu_1+1}{2}}m^{\frac{1-\mu_1}{2}}\gamma_1 - 2, 2^{\frac{\mu_2+1}{2}}\gamma_2 - 2, \frac{1}{\tau_i}2^{\frac{\mu_1+1}{2}}m^{\frac{1-\mu_1}{2}} - 2, \frac{1}{\tau_i}2^{\frac{\mu_2+1}{2}} - 2, \vartheta_i\psi\}$. The penult inequality is based on the fact that $y \leqslant y^{\mu_1} + y^{\mu_2}$ holds for some positive constant $y$.

It yields that

$$
V_4 \leqslant \frac{Q_1}{\xi_1} + (V_4(t_0) - \frac{Q_1}{\xi_1})e^{-\xi_1(t-t_0)}. \tag{56}
$$

From inequality (56), we can obtain that all variables $e_{xi}, \bar{e}_{vi}, \tilde{\sigma}_i$ and $\tilde{\theta}_i$ are UUB.

**Step 2.** According to Step 1, $\|\tilde{\theta}_i\|_2 \leqslant \tilde{\theta}_{Mi}$ holds for some positive constant $\tilde{\theta}_{Mi}$. Moreover, from Theorem 1, $\varepsilon_{xi} = \varepsilon_{vi} = \tilde{z}_v = 0$ for all $t \geqslant T_0$. Thus, for $t \geqslant T_0$, we have:

$$\begin{aligned}\dot{V}_4 \leqslant\ & -(2^{\frac{\mu_1+1}{2}} m^{\frac{1-\mu_1}{2}}\lambda_1 - 2)(\tfrac{1}{2}e_{xi}^T e_{xi})^{\frac{\mu_1+1}{2}} \\ & -(2^{\frac{\mu_2+1}{2}}\lambda_2 - 2)(\tfrac{1}{2}e_{xi}^T e_{xi})^{\frac{\mu_2+1}{2}} \\ & -(2^{\frac{\mu_1+1}{2}} m^{\frac{1-\mu_1}{2}}\gamma_1 - 1)(\tfrac{1}{2}\bar{e}_{vi}^T \bar{e}_{vi})^{\frac{\mu_1+1}{2}} \\ & -(2^{\frac{\mu_2+1}{2}}\gamma_2 - 1)(\tfrac{1}{2}\bar{e}_{vi}^T \bar{e}_{vi})^{\frac{\mu_2+1}{2}} \\ & -(\tfrac{1}{\tau_i}2^{\frac{\mu_1+1}{2}} m^{\frac{1-\mu_1}{2}} - 2)(\tfrac{1}{2}\tilde{\sigma}_i^T\tilde{\sigma}_i)^{\frac{\mu_1+1}{2}} \\ & -(\tfrac{1}{\tau_i}2^{\frac{\mu_2+1}{2}} - 2)(\tfrac{1}{2}\tilde{\sigma}_i^T\tilde{\sigma}_i)^{\frac{\mu_2+1}{2}} + Q_2 \\ & -(\tfrac{1}{2}\mathrm{tr}(\tilde{\theta}_i^T\psi_i^{-1}\tilde{\theta}_i))^{\frac{\mu_1+1}{2}} - (\tfrac{1}{2}\mathrm{tr}(\tilde{\theta}_i^T\psi_i^{-1}\tilde{\theta}_i))^{\frac{\mu_2+1}{2}}.\end{aligned} \tag{57}$$

where $Q_2 = -\frac{1}{2}\vartheta_i\mathrm{tr}(\tilde{\theta}_i^T\tilde{\theta}_i) + (\frac{1}{2}\mathrm{tr}(\tilde{\theta}_i^T\psi_i^{-1}\tilde{\theta}_i))^{\frac{\mu_1+1}{2}} + \frac{1}{2}\sigma_{Mi} + \frac{1}{2}\vartheta_i\theta_M^2 + \frac{1}{2}\varepsilon_M^2 + (\frac{1}{2}\mathrm{tr}(\tilde{\theta}_i^T\psi_i^{-1}\tilde{\theta}_i))^{\frac{\mu_2+1}{2}}$.

Since $\tilde{\theta}_i$ is UUB from Step 1, we can get that $-\frac{1}{2}\vartheta_i\mathrm{tr}(\tilde{\theta}_i^T\tilde{\theta}_i) + (\frac{1}{2}\mathrm{tr}(\tilde{\theta}_i^T\psi_i^{-1}\tilde{\theta}_i))^{\frac{\mu_1+1}{2}} + (\frac{1}{2}\mathrm{tr}(\tilde{\theta}_i^T\psi_i^{-1}\tilde{\theta}_i))^{\frac{\mu_2+1}{2}} \leqslant \bar{\theta}_{Mi}$ holds for a positive constant $\bar{\theta}_{Mi}$. Then, (57) can be rewritten as

$$\begin{aligned}\dot{V}_4 \leqslant\ & -c_1(\tfrac{1}{2}e_{xi}^T e_{xi})^{\frac{\mu_1+1}{2}} + (\tfrac{1}{2}\bar{e}_{vi}^T\bar{e}_{vi})^{\frac{\mu_1+1}{2}}) \\ & -c_1((\tfrac{1}{2}\tilde{\sigma}_i^T\tilde{\sigma}_i)^{\frac{\mu_1+1}{2}} + (\tfrac{1}{2}\mathrm{tr}(\tilde{\theta}_i^T\psi_i^{-1}\tilde{\theta}_i))^{\frac{\mu_1+1}{2}}) \\ & -c_2((\tfrac{1}{2}e_{ix}^T e_{xi})^{\frac{\mu_2+1}{2}} + (\tfrac{1}{2}\bar{e}_{vi}^T\bar{e}_{vi})^{\frac{\mu_2+1}{2}}) \\ & -c_2((\tfrac{1}{2}\tilde{\sigma}_i^T\tilde{\sigma}_i)^{\frac{\mu_2+1}{2}} + (\tfrac{1}{2}\mathrm{tr}(\tilde{\theta}_i^T\psi_i^{-1}\tilde{\theta}_i))^{\frac{\mu_2+1}{2}}) + Q_2 \\ \leqslant\ & -2^{1-\mu_1}c_1(V_4)^{\frac{\mu_1+1}{2}} - c_2(V_4)^{\frac{\mu_2+1}{2}} + Q_2,\end{aligned} \tag{58}$$

where $c_1 = \min\{2^{\frac{\mu_1+1}{2}}m^{\frac{1-\mu_1}{2}}\lambda_1 - 2, 2^{\frac{\mu_1+1}{2}}m^{\frac{1-\mu_1}{2}}\gamma_1 - 1, \frac{1}{\tau_i}2^{\frac{\mu_1+1}{2}}m^{\frac{1-\mu_1}{2}} - 1, 1\}$ and $c_2 = \min\{2^{\frac{\mu_2+1}{2}}\gamma_2 - 2, 2^{\frac{\mu_2+1}{2}}\gamma_2 - 1, \frac{1}{\tau_i}2^{\frac{\mu_2+1}{2}} - 1, 1\}$.

According to Lemma 2.2 in [27], we can obtain that $X_i = [e_{xi}^T, \bar{e}_{vi}^T, \tilde{\sigma}_i^T]^T$ is practical fixed-time stable and will converge to the compact set $\Pi$ within fixed time $\bar{T}_0 \leqslant \frac{2^{\mu_1}}{(\mu_1-1)c_1\phi} + \frac{2}{c_2\phi(1-\mu_2)} + T_0$, where

$$\begin{aligned}\Pi = \{X_i | V_4(X_i) \\ \leqslant \min\{(\frac{Q_2}{(1-\phi)c_1}2^{\mu_1-1})^{\frac{2}{\mu_1+1}}, (\frac{Q_2}{(1-\phi)c_2})^{\frac{2}{\mu_2+1}}\}\}.\end{aligned} \tag{59}$$

Since $\delta_{xi} = e_{xi}$ and $\delta_{vi} = e_{vi}$ for $t \geqslant T_0, \delta$ can converge to a small compact set in fixed time $\bar{T}_0$ by appropriately choosing the control and adaptive parameters as well. Consequently, the MASs are able to realize the desired time-varying formation in fixed time $\bar{T}_0$. This completes the proof.

**Remark 5.** By means of designing the nonlinear nonsmooth filter (42), the explosion of complexity problem brought from the backstepping technique is well solved. Moreover, in comparison with the first-order traditional filters, filter (42) can guarantee the fixed-time convergence of the filtering errors.

**Remark 6.** In fact, the followers and leader work with limited energy. As an efficient method to reduce communication and energy consumption, event-triggered strategy is widely utilized in the control systems [28,33,38–44]. Thus, in our future work, we will further try to combine the proposed formation control scheme with event-triggered mechanism in the above literatures under directed topologies such that the proposed control scheme is more practical. In addition, measurement incompleteness problem [45] also deserves deep research. Therefore, we will also try to take measurement incompleteness problem into consideration in the formation tracking control design and analysis in the future.

## 4. Simulation

To verify the effectiveness of the proposed formation control scheme, we establish a MAS consisting of six followers and one leader, whose dynamics are described by (1) and (2), respectively. Choose the graph $G_0$ as the topology graph, which is shown in Fig. 2. From Fig. 2, the graph $G_0$ is a directed graph having a spanning tree. In addition, for the 1st and 6th followers, $\sum_{j=1}^N a_{1j} = \sum_{j=1}^N a_{6j} = 0$, which satisfies the condition of Assumption 1.

In this simulation, the six followers are supposed to form and maintain a time-varying regular hexagon formation of which edges lengthen along with time in the X-Y plane and to rotate around the varying leader with $x_0 = [5\cos(0.1t), 5t]^T$ simultaneously.

Moreover, the uncertainties $f_i$ are selected as

$$\begin{aligned} f_1 &= [3\sin(0.2v_{1X}), 2\cos(0.1v_{1Y})]^T, \\ f_2 &= [3\cos(0.2v_{2X}), 2\cos(0.2v_{2Y})]^T, \\ f_3 &= [3\sin(0.1v_{3X}^2), 2\cos(0.1v_{3Y}^2)]^T, \\ f_4 &= [3\sin(0.1v_{4X}^2), 2\cos(0.1v_{4Y}^2)]^T, \\ f_5 &= [3\sin(0.1v_{5X}^2), 2\sin(0.1v_{5Y}^2)]^T, \\ f_6 &= [3\sin(0.2v_{6X}^2), 2\cos(0.1v_{6Y}^2)]^T, \end{aligned} \tag{60}$$

where $v_{iX}$ and $v_{iY}$ denote the elements of the vector $v_i = [v_{iX}, v_{iY}]^T$. Moreover, $h_{xi}$ is given as follows

$$h_{xi}(t) = \begin{bmatrix} 0.2t\cos(0.1t + (i-1)\pi/3) \\ 0.2t\sin(0.1t + (i-1)\pi/3) \end{bmatrix}. \tag{61}$$

In addition, the values of the observer and control parameters are set as shown in Tables 1 and 2, respectively. We choose the initial position states of the six followers and the leader as $x_1(0) = [5,5]^T,\ x_2(0) = [0,-4]^T,\ x_3(0) = [-4,4]^T,$ $x_4(0) = [3,3]^T,\ x_5(0) = [5,2]^T,\ x_6(0) = [1,-3]^T,\ x_0(0) = [0,10]^T,$ while the initial velocity state vectors of those are chosen as zero vectors. Figs. 3–7 show the simulation results. Fig. 3 presents the varying positions at $t = 10, 15, 20, 25, 30$ s, from which we can observe that the six followers achieve the desired time-varying regular hexagon formation with the length of its edges growing longer. Moreover, the six followers track the trajectory of the dynamic leader in the meanwhile. Fig. 4 depicts the curves of $\delta_{xi}$ along X-axis and Y-axis. Fig. 5 represents the curves of the observation errors $\tilde{x}_{0i}$ and $\tilde{\bar{v}}_{0i}$ along X-axis and Y-axis. From Figs. 4,5, we can get that the formation tracking error $\delta_{xi}$ can converge to a small enough neighborhood of the origin in 5 s, while $\tilde{x}_{0i}$ and $\tilde{\bar{v}}_{0i}$

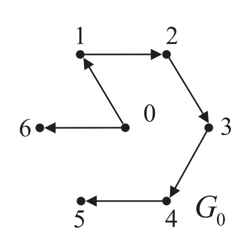


**Fig. 2.** The interaction graph.

**Table 1**
Control parameters.

| $\lambda_1$ | $\lambda_2$ | $\gamma_1$ | $\gamma_2$ | $\mu_1$ | $\mu_2$ | $\tau_i$ | $\psi_i$ |
|---|---|---|---|---|---|---|---|
| 2 | 3 | 2 | 1 | 1.5 | 0.8 | 0.5 | 0.01 |
| $\vartheta_1$ | $\vartheta_2$ | $\vartheta_3$ | $\vartheta_4$ | $\vartheta_5$ | $\vartheta_6$ | | |
| 2 | 2 | 2 | 2 | 1 | 1 | | |

**Table 2**
Observer parameters.

| $\alpha_1$ | $\alpha_2$ | $\beta_1$ | $\beta_2$ | $m_1$ | $m_2$ | $m_3$ | $m_4$ |
|---|---|---|---|---|---|---|---|
| 10 | 10 | 0.1 | 0.1 | 0.95 | 1.05 | 0.9 | 1.1 |
| $\kappa_x$ | $\kappa_v$ | $\rho_x$ | $\rho_v$ | $q_1$ | $q_2$ | | |
| 1 | 1 | 1 | 2 | 2 | 0.5 | | |

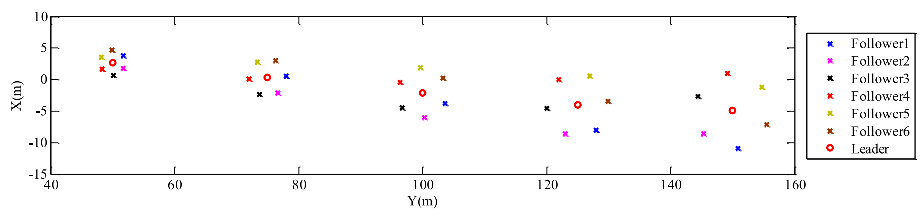


**Fig. 3.** Position snapshots of the six followers and the leader.

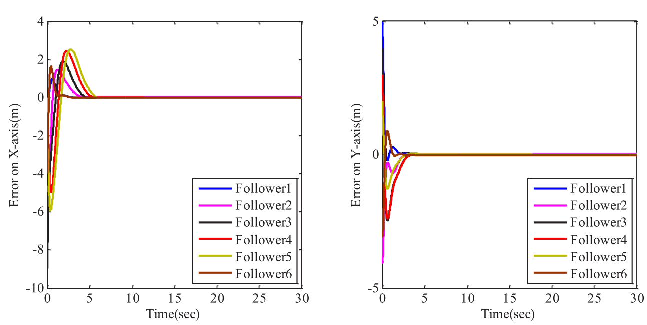


**Fig. 4.** Formation tracking position errors on X-axis and Y-axis of the six followers.

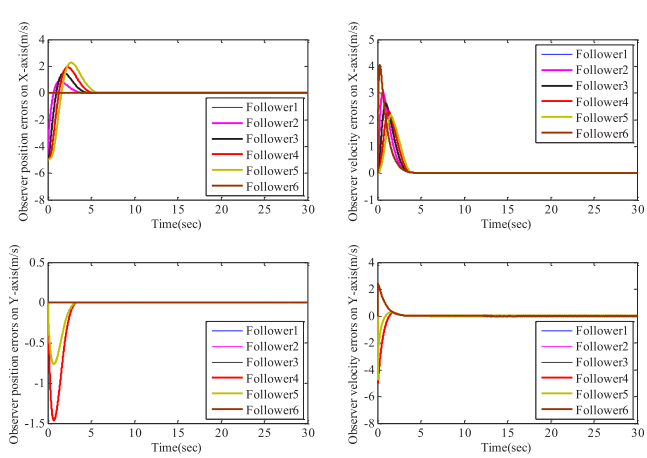


**Fig. 5.** Observation errors of the six followers on X-axis and Y-axis.

converge to the origin at around 3 s. Figs. 6 and 7 display the curves of the MLP outputs and the control inputs along X-axis and Y-axis, respectively.

Moreover, we conduct another simulation under different initial states of the six followers to verify the fixed-time convergence

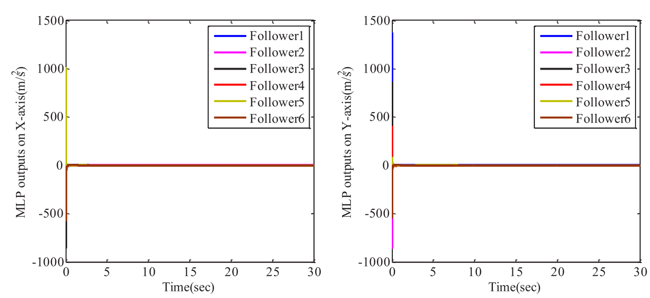


**Fig. 6.** MLP outputs on X-axis and Y-axis of the six followers.

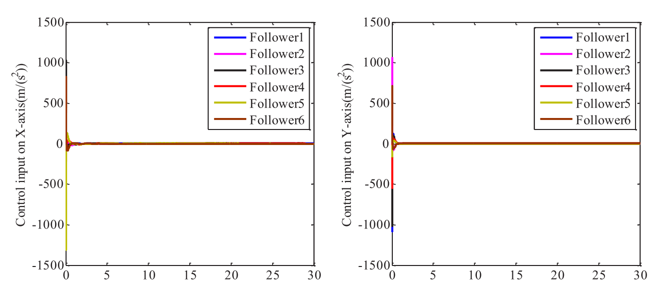


**Fig. 7.** Control inputs on X-axis and Y-axis of the six followers.

of the formation tracking errors. Fig. 8 presents the formation tracking position errors on X-axis and Y-axis of the six followers under initial states $x_1(0) = [10, -10]^T$, $x_2(0) = [-5, 10]^T$, $x_3(0) = [0, -8]^T$, $x_4(0) = [-6, -6]^T$, $x_5(0) = [-10, -4]^T$, $x_6(0) = [6, 6]^T$. From Figs. 4 and 8, we can get that the formation tracking position errors converge in a similar settling time. Since the obvious feature of fixed-time control is that the settling time is independent of the initial states, we can draw a conclusion that the formation position errors can converge in a fixed time under the proposed fixed-time formation control scheme.

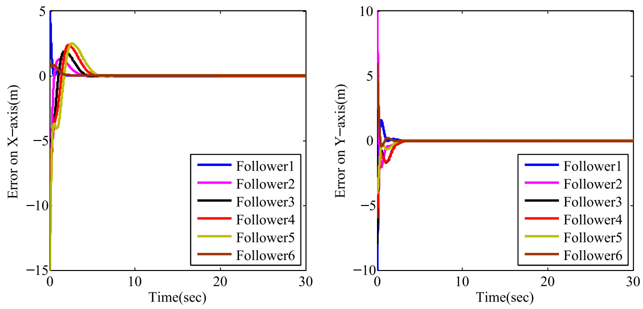


**Fig. 8.** Formation tracking position errors on X-axis and Y-axis of the six followers under different initial states.

## 5. Conclusion

In order to cope with the time-varying formation tracking control problem in a fixed time for MASs in presence of uncertainties under directed topologies and with no need for LVMs, an observer based adaptive fixed-time formation control scheme with MLP is established in this paper. A new CFTSO is put forward to ensure that each follower can acquire the estimates of the LSs within a fixed time under directed topologies, which overcomes the difficulty of the absence of the LVMs. By utilizing MLP technique, the model uncertainties are well addressed and the computation burden is lighted at the same time. The strict stability analysis is presented and the effectiveness of the proposed control scheme is validated by the simulation results. In our future work, we will do our best to achieve the fixed-time formation tracking for multi-agent systems under directed topologies in the event-triggered control framework. In addition, we will also explore the measurement incompleteness problem and achieve expected formation tracking in the meantime.

## CRediT authorship contribution statement

**Tianyi Xiong:** Conceptualization, Methodology, Software, Writing - original draft. **Zhou Gu:** Supervision, Formal analysis, Funding acquisition. **Jianqiang Yi:** Investigation, Validation. **Zhiqiang Pu:** Writing - review & editing.

## Declaration of Competing Interest

The authors declare that they have no known competing financial interests or personal relationships that could have appeared to influence the work reported in this paper.

## Acknowledgment

This work was supported by the National Natural Science Foundation of China under Grant 62022044 and 61473-156, in part by the Jiangsu Natural Science Foundation for Distinguished Young Scholars under Grant BK20190039.

## References

[1] Y. Wang, L. Cheng, Z. Hou, J. Yu, M. Tan, Optimal formation of multirobot systems based on a recurrent neural network, IEEE Trans. Neural Networks Learn. Syst. 27 (2) (2016) 322–333.
[2] J. Wang, X. Ma, H. Li, B. Tian, Self-triggered sliding mode control for distributed formation of multiple quadrotors, J. Franklin Inst. 357 (17) (2020) 12223–12240.
[3] X. Ge, Q. Han, X. Zhang, Achieving cluster formation of multi-agent systems under aperiodic sampling and communication delays, IEEE Trans. Ind. Electron. 65 (4) (2018) 3417–3426.
[4] X. Dong, G. Hu, Time-varying formation control for general linear multi-agent systems with switching directed topologies, Automatica 73 (2016) 47–55.
[5] R. Wang, X. Dong, Q. Li, Z. Ren, Distributed time-varying formation control for multiagent systems with directed topology using an adaptive output-feedback approach, IEEE Trans. Ind. Inf. 15 (8) (2019) 4676–4685.
[6] L. Han, Y. Xie, X. Li, X. Dong, Q. Li, Z. Ren, Time-varying group formation tracking control for second-order multi-agent systems with communication delays and multiple leaders, J. Franklin Inst. 357 (14) (2020) 9761–9780.
[7] A. Polyakov, Nonlinear feedback design for fixed-time stabilization of linear control systems, IEEE Trans. Autom. Control 57 (8) (2012) 2106–2110.
[8] Z. Zuo, Q. Han, B. Ning, X. Ge, X. Zhang, An overview of recent advances in fixed-time cooperative control of multiagent systems, IEEE Trans. Ind. Inf. 14 (6) (2018), 2322–2234.
[9] J. Ni, Y. Tang, P. Shi, A new fixed-time consensus tracking approach for second-order multiagent systems under directed communication topology, IEEE Trans. Syst. Man Cybern. Syst. 51 (4) (2021) 2488–2500.
[10] Z. Zuo, B. Tian, M. Defoort, Z. Ding, Fixed-time consensus tracking for multiagent systems with high-order integrator dynamics, IEEE Trans. Autom. Control 63 (2) (2018) 563–570.
[11] T. Xiong, Z. Pu, J. Yi, X. Tao, Fixed-time observer based adaptive neural network time-varying formation tracking control for multi-agent systems via minimal learning parameter approach, IET Control Theory Appl. 14 (9) (2020) 1147–1157.
[12] T. Xiong, Z. Gu, Observer-based adaptive fixed-time formation control for multi-agent systems with unknown uncertainties, Neurocomputing 423 (2021) 506–517.
[13] X. Liang, H. Wang, Y. Liu, W. Chen, T. Liu, Formation control of nonholonomic mobile robots without position and velocity measurements, IEEE Trans. Rob. 34 (2) (2018) 434–446.
[14] T. Sun, F. Liu, H. Pei, Y. He, Observer-based adaptive leader-following formation control for non-holonomic mobile robots, IET Control Theory Appl. 6 (18) (2012) 2835–2841.
[15] J. Fu, J. Wang, Fixed-time coordinated tracking for second-order multi-agent systems with bounded input uncertainties, Syst. Control Lett. 93 (2016) 1–12.
[16] X. Wu, S. Wang, M. Xing, Observer-based leader-following formation control for multi-robot with obstacle avoidance, IEEE Access 7 (2019) 14791–14798.
[17] Z. Zuo, M. Defoort, B. Tian, Z. Ding, Distributed consensus observer for multi-agent systems with high-order integrator dynamics, IEEE Trans. Autom. Control 65 (4) (2020) 1771–1778.
[18] X. Tao, J. Yi, Z. Pu, T. Xiong, State-estimator-integrated robust adaptive tracking control for flexible air-breathing hypersonic vehicle with noisy measurements, IEEE Trans. Instrum. Meas. 68 (11) (2019) 4285–4299.
[19] E. Tian, Z. Wang, L. Zou, D. Yue, Chance-constrained $H_\infty$ control for a class of time-varying systems with stochastic nonlinearities: The finite-horizon case, Automatica 107 (2019) 296–305.
[20] Z. Pu, J. Sun, J. Yi, Z. Gao, On the principle and applications of conditional disturbance negation, IEEE Trans. Syst. Man Cybern. Syst. to be published. doi:10.1109/TSMC.2020.2964045..
[21] X. Liu, S.S. Ge, C. Goh, Neural-network-based switching formation tracking control of multiagents with uncertainties in constrained space, IEEE Trans. Syst. Man Cybern. Syst. 49 (5) (2019) 1006–1015.
[22] L. Zhao, Y. Jia, Neural-network-based distributed adaptive attitude synchronization control of spacecraft formation under modified fast terminal sliding mode, Neurocomputing 171 (C) (2016) 230–241..
[23] Y. Zhang, J. Sun, H. Liang, H. Li, Event-triggered adaptive tracking control for multiagent systems with unknown disturbances, IEEE Trans. Cybern. 50 (3) (2020) 890–901.
[24] J. Qin, G. Zhang, W. Zheng, Y. Kang, Neural network-based adaptive consensus control for a class of nonaffine nonlinear multiagent systems with actuator faults, IEEE Trans. Neural Networks Learn. Syst. 30 (12) (2019) 3633–3644.
[25] X. Bu, X. Wu, J. Huang, Z. Ma, R. Zhang, Minimal-learning-parameter based simplified adaptive neural back-stepping control of flexible air-breathing hypersonic vehicles without virtual controllers, Neurocomputing 175 (2016) 816–825.
[26] X. Tao, J. Yi, Z. Pu, T. Xiong, Robust adaptive tracking control for hypersonic vehicle based on interval type-2 fuzzy logic system and small-gain approach, IEEE Trans. Cybern. 51 (5) (2021) 2504–2517.
[27] D. Ba, Y. Li, S. Tong, Fixed-time adaptive neural tracking control for a class of uncertain nonstrict nonlinear systems, Neurocomputing 363 (2019) 273–280.
[28] J. Ni, P. Shi, Y. Zhao, Q. Pan, S. Wang, Fixed-time event-triggered output consensus tracking of high-order multiagent systems under directed interaction graphs, IEEE Trans. Cybern. to be published. doi:10.1109/TCYB.2020.3034013..
[29] Z. Zuo, Nonsingular fixed-time consensus tracking for second-order multi-agent networks, Automatica 54 (2015) 305–309.
[30] B. Tian, H. Lu, Z. Zuo, W. Yang, Fixed-time leader-follower output feedback consensus for second-order multiagent systems, IEEE Trans. Cybern. 49 (4) (2019) 1545–1550.
[31] T. Xiong, Z. Gu, Observer-based fixed-time consensus control for nonlinear multi-agent systems subjected to measurement noises, Neurocomputing 8 (2020) 174191–174199.
[32] J. Ni, P. Shi, Adaptive neural network fixed-time leader–follower consensus for multiagent systems with constraints and disturbances, IEEE Trans. Cybern. 51 (4) (2021) 1835–1848.
[33] J. Liu, Y. Zhang, Y. Yu, C. Sun, Fixed-time leader-follower consensus of networked nonlinear systems via event/self-triggered control, IEEE Trans. Neural Networks Learn. Syst. 31 (11) (2020) 5029–5037.

[34] M.V. Basin, P. Yu, Y.B. Shtessel, Hypersonic missile adaptive sliding mode control using finite- and fixed-time observers, IEEE Trans. Ind. Electron. 65 (1) (2018) 930–941.
[35] J. Sun, Z. Pu, J. Yi, Z. Liu, Fixed-time control with uncertainty and measurement noise suppression for hypersonic vehicles via augmented sliding mode observers, IEEE Trans. Ind. Inf. 16 (2) (2020) 1192–1203.
[36] J. Sun, J. Yi, Z. Pu, X. Tan, Fixed-time sliding mode disturbance observer-based nonsmooth backstepping control for hypersonic vehicles, IEEE Trans. Syst. Man Cybern. Syst. 20 (11) (2020) 4377–4386.
[37] J. Li, Y. Yang, C. Hua, X. Guan, Fixed-time backstepping control design for high-order strict-feedback non-linear systems via terminal sliding mode, IET Control Theory Appl. 11 (8) (2017) 1184–1193.
[38] B. Zhang, Q. Han, X. Zhang, Event-triggered $H_\infty$ reliable control for offshore structures in network environments, J. Sound Vib. 368 (2016) 1–21.
[39] Z. Gu, D. Yue, E. Tian, On designing of an adaptive event-triggered communication scheme for nonlinear networked interconnected control systems, Inf. Sci. 422 (2018) 257–270.
[40] J. Liu, Y. Zhang, Y. Yu, C. Sun, Fixed-time event-triggered consensus for nonlinear multiagent systems without continuous communications, IEEE Trans. Syst. Man Cybern. Syst. 49 (11) (2019) 2221–2229.
[41] X. Ge, Q. Han, L. Ding, Y. Wang, X. Zhang, Dynamic event-triggered distributed coordination control and its applications: A survey of trends and techniques, IEEE Trans. Syst. Man Cybern. Syst. 50 (9) (2020) 3112–3125.
[42] B. Zhang, E. Cao, Z. Cai, H. Su, G. Tang, Event-triggered $H_\infty$ control for networked spar-type floating production platforms with active tuned heave plate mechanisms and deception attacks, J. Franklin Inst. 358 (7) (2021) 3554–3584.
[43] Z. Gu, J. H. Park, D. Yue, Z. Wu, X. Xie, Event triggered security output feedback control for networked interconnected systems subject to cyber-attacks, IEEE Trans. Syst. Man Cybern. Syst. to be published. doi:10.1109/TSMC.2019.2960115..
[44] X. Ge, Q. Han, Z. Wang, A dynamic event-triggered transmission scheme for distributed set-membership estimation over wireless sensor networks, IEEE Trans. Cybern. 49 (1) (2019) 171–183.
[45] B. Shen, Z. Wang, H. Qiao, Event-triggered state estimation for discrete-time multidelayed neural networks with stochastic parameters and incomplete measurements, IEEE Trans. Neural Networks Learn. Syst. 28 (5) (2017) 1152–1163.

**Tianyi Xiong** received the Ph.D degree from Institute of Automation, Chinese Academy of Sciences in 2019 and the B.S. and M.S. degrees from Harbin Institute of Technology, in 2014 and 2016, respectively. She is currently a postdoctoral researcher with Nanjing Forestry University, Nanjing, China. Her current research interests include formation control, fixed-time control and network control systems.

**Zhou Gu** received the B.S. degree from North China Electric Power University, Beijing, China, in 1997 and the M.S. and Ph.D. degrees in control science and engineering from Nanjing University of Aeronautics and Astronautics, Nanjing, China, in 2007 and 2010, respectively. From September 1996 to January 2013, he was with the School of Power engineering, Nanjing Normal University as an associate professor. He was a visiting scholar with Central Queensland University, Rockhampton, Queensland, Australia and The University of Manchester, Manchester, U.K. He is currently a Professor with Nanjing Forestry University, Nanjing, China. His current research interests include networked control systems, time-delay systems, reliable control and their applications.

**Jianqiang Yi** received the B.Eng. degree in mechanical engineering from Beijing Institute of Technology, Beijing, China, in 1985, and the M.Eng. and Ph.D. degrees in automation from the Kyushu Institute of Technology, Kitakyushu, Japan, in 1989 and 1992, respectively.
From 1992 to 1994, he worked as a Research Fellow with the Computer Software Development Company, Tokyo, Japan. From 1994 to 2001, He was a Chief Engineer with MYCOM, Inc., Kyoto, Japan. Since 2001, he has been a Full Professor with the Institute of Automation, Chinese Academy of Sciences, Beijing, China. He has authored or co-authored over 100 international journal papers and 240 international conference papers. He holds more than 40 issued domestic patents. His research interests include theories and engineering applications of intelligent control, adaptive control, and intelligent robotics.
Prof. Yi was an Associate Editor of *IEEE Computational Intelligence Magazine* from 2008 to 2009, and is an Associate Editor for the *Journal of Advanced Computational Intelligence and Intelligent Informatics*, and *International Journal of Innovative Computing, Information and Control*.

**Zhiqiang Pu** received the B.Eng. degree in automation from Wuhan University, Wuhan, China, in 2009, and the Ph.D. degree in control theory and control engineering from Institute of Automation, Chinese Academy of Sciences, Beijing, China, in 2014.
He is currently an Associate Professor with the Integrated Information System Research Center, Institute of Automation, Chinese Academy of Sciences. He has been supported by the Talent Program of Youth Innovation Promotion Association, Chinese Academy of Sciences, since 2017.
His research interests include nonlinear control, robust adaptive control, swarm robotics, and unmanned autonomous systems.